JOURNAL OF Materials Feature Article CHEMISTRY

Inorganic lyotropic liquid crystals

A. S. Sonin

A. I. Nesmeyanov Institute of Elemento-Organic Compounds, Russian Academy of Sciences, Vavilova Str. 28, 117813 Moscow, Russia

Received 7th April 1998, Accepted 5th May 1998

A detailed review of inorganic lyotropic liquid crystals (water or water–organic dispersions of certain non-organic substances) is presented. The history of the discovery of these mesophases is described and their classification is considered. The structure and properties of all liquid crystals of this class known to date are analysed in detail.

Introduction

Liquid crystals were discovered among organic compounds more than a century ago. In the beginning, mesophases were found by melting of cholesterol ethers and nitro compounds,[1] and later by dissolving the long-chain acid salts.[2] The former substances were named 'thermotropic', and the latter 'lyotropic' liquid crystals. These mesophases were found to exhibit orientational order in a certain range of temperatures (for thermotropic substances) and/or concentrations (for lyotropic ones).[3]

Over the following century more than 10 000 different liquid crystals were discovered. The great majority of these substances are organic compounds with highly variable chemical compositions. This circumstance usually does not provoke any misunderstanding, since one of the necessary conditions of the mesomorphism—the anisosymmetry of molecules—may, in fact, be most easily realised in organic compounds.

The anisosymmetry of forms of the structural units is equally necessary for formation of both thermotropic and lyotropic mesophases. Separate molecules usually serve as structural units for thermotropic liquid crystals, while molecular aggregates (micelles and columns) usually play this role for lyotropic liquid crystals. In some cases, the structural units may be represented by single molecules of quite large size, oligomers and living organisms (viruses). Such systems are typically colloidal.

In addition, there are quite a lot of colloidal systems with non-organic dispersion phases. Therefore, it should be logical to expect that, if a non-organic dispersive phase of this kind consists of anisometric particles, then such a colloidal system will exhibit liquid-crystalline properties.

History

The historical idea of the possibility of existence of inorganic liquid crystals was formed gradually, mainly due to studies of induced optical anisotropy in sols. This is the so-called Majorana effect, which manifested itself by the appearance of a birefringence in some sols under the action of a magnetic field[4] (Majorana himself worked with FeOOH). The studies of this phenomenon[5–9] showed that sols consisting of anisometric particles can be orientationally ordered under the action of a magnetic field. However, after switching off the magnetic field, the orientational order was destroyed by thermal motion.

A second way to obtain induced optical anisotropy of sols—orientation by flow—was found in 1915.[10] It was shown that sols of vanadium pentoxide (V_2O_5) acquired strong birefringence when a flow was created in this dispersion by shaking of a retort or by the sol preparation.

Soon afterwards, Freundlich showed[11] that V_2O_5 sols also become optically anisotropic in electric fields. Moreover, he proved[11,12] that the Majorana effect and the appearance of optical anisotropy in an electric field and under a flow was caused by the same reason—the orientation of the anisometrical particles with their long axes in the direction of the flow or of the electric and magnetic field strength. The sol samples were found to behave like optically uni-axial positively charged crystals with considerable dichroism. After switching off the orientation-inducing action, the sols returned to their initial optically isotropic state.

It was possible to observe the V_2O_5 sol particles with the help of an ultramicroscope. They had the appearance of long sticks, with the length-to-width ratio equal to approximately 10 : 1. Freundlich called these particles 'swarms', in analogy with 'swarms' in liquid crystals, the existence of which was considered to be proved at this time.

The analogy between sols with induced optical anisotropy and thermotropic liquid crystals was specially discussed by Freundlich.[11,12] He also pointed out the 'similarity' of both phenomena, since liquid crystals were found to behave in a magnetic field analogously to sols. However, he stressed that there were considerable differences between these two classes of substances. Firstly, thermotropic liquid crystals are single-phase systems, while sols are two-component compounds. Secondly, liquid crystals form homogeneously oriented, optically anisotropic samples between two glass walls in a plane-parallel capillary, while sols do not form such samples. Thirdly, in the initial state, sols are transparent, while liquid crystals are opaque. Fourthly, sols acquire an optical anisotropy when flowing, while thermotropic liquid crystals of *p*-azoxyanisol and *p*-azoxyphenol, as the Freundlich experiments showed, do not exhibit any anisotropy.† However, he observed optical birefringence in homeotropic samples of these substances, upon displacing the upper glass of a cell.

From all the results mentioned above, Freundlich made the following prudent statement: 'Everybody now comes to the conclusion that the V_2O_5 sol, in general, from different points of view, is the magnified model of an anisotropic melt (*i.e.* of a thermotropic liquid crystal—A.S.)'.[11]

The question of the nature of the ordered particles—the structural units of sols—had already arisen in these pioneering works. This issue was discussed during the debates on the Freundlich report at the meeting of the German Electrochemical Society.[11] Freundlich himself considered this question to be unclear, since in spite of the proven (by the microscopic observations) crystalline nature of these particles, some amorphous residue appeared during coagulation. However, this fact, as it was pointed out by Zigmondi,[11] did not contradict the statement about the crystalline character of the sol particles. He insisted on this latter statement.

† In reality, as shown by Zöcher,[15] thermotropic liquid crystals can be oriented by a flow, and, then, their optical anisotropy increases.

The ultramicroscopy studies[13,14] proved, in general, the Zigmondi point of view. It was shown that, in the V_2O_5 sols, the structural units were elongated particles of a clearly crystalline character, with length 7 μm and width 0.5–2 μm. The particle length reached up to 19 μm in old sols (3.5 years). In an isotropic sol these particles were not situated chaotically, but in small areas were oriented parallel to each other, without intersections.

The particle forms and sizes were also determined by means of an ultramicroscope in some other sols (mercury chloride, HgCl; lead iodide, PbI_2) exhibiting birefringence in a flow. It was shown that in the first sol they were puck-shaped with a diameter of about 1 μm, while in the second sol they were needle-shaped with lengths between 0.25 and 2 μm.

Inorganic sols with induced optical anisotropy were further investigated in detail by Zöcher *et al.*[15,16] They found the appearance of birefringence in flowing sols of AgCNO, in a clay suspension and in a sequence of mesogenic organic compounds.[15] V_2O_5 was studied quantitatively in detail.[16–18] The dependences of birefringence and dichroism upon the flow rate, temperature, sol concentration and age were measured in a pipe with a rectangular cross-section and between turning cylinders. The essential result was the proof of the fact that the freshly prepared V_2O_5 sol did not exhibit induced birefringence; however, the birefringence developed with time. The ageing velocity was found to be described by a second order equation. This velocity increased sharply with increasing temperature. The induced birefringence increased linearly with increasing flow rate and decreased linearly with increasing temperature.

It was found, while studying induced birefringence,[19] that old V_2O_5 sols began to rearrange into layered structures as time passed. The upper sol part (about two thirds of a sample) remained isotropic, while the lower part became strongly birefringent. At the same time, the concentration of the substance in the lower part increased, while in the upper part it decreased. Thus, a sol having an initial concentration of 1.43 mass%, after 9 days became arranged in layers so that the concentration in its upper part became 2.14 mass%, and that in its lower part became 1.39 mass%.[20]

If one mixes drops of the upper and lower phases, and observes the obtained isotropic sample under a polarising microscope, after 0.5–2 hours the optically anisotropic areas—linear areas of a spindle-like form, named tactoids[20]—will appear in a sample.[20–24] They are clearly distinguished in the polarised-light micrographs (Fig. 1).

Anisotropic areas, analogous in many features to tactoids, are also found in other inorganic sols: H_2WO_4[20] and FeOOH.[21]‡ The latter, in contrast to V_2O_5, possesses rainbow colours. This is due to the layered structure of such sols—the distance between these layers is of the order of magnitude of the wavelength of visible light.[21] This layered character is clearly visible in Fig. 2, where a micrograph of a 5 mass%, 15 year old FeOOH sol is presented. This micrograph is surprisingly similar to the textures of smectic drops with steps. The latter are reproduced in numerous textbooks on liquid crystals as proof of the layered structure of smectics.

The V_2O_5 tactoids, in contrast, look like nematic drops nucleating in an isotropic melt. However, in thermotropic nematics, such drops have a spherical form; nevertheless, the optical anisotropy of tactoids leaves no doubt concerning the similarity of these structures to those of nematic liquid crystals.

In spite of that fact, Zöcher and his co-authors did not venture to identify, in their early works on tactoids, anisotropic inorganic sols (they were called tactosols) with liquid crystals. This is what Zöcher, himself, wrote in this connection in his

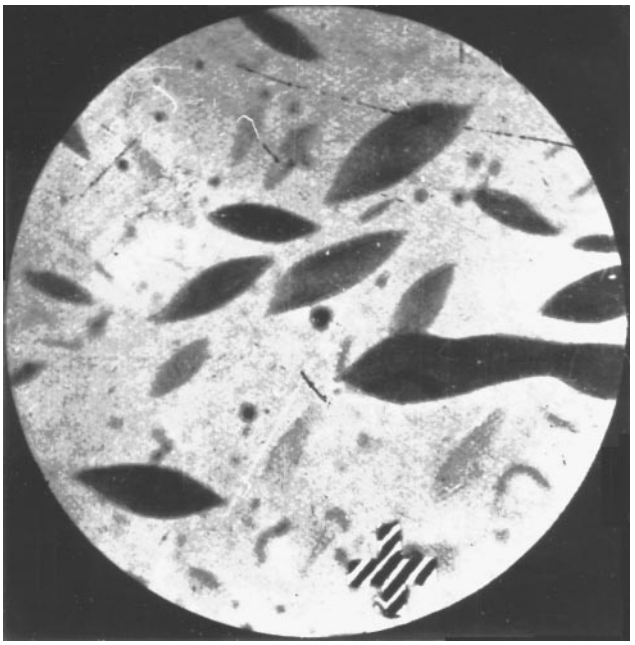

Fig. 1 Tactoids in a vanadium pentoxide dispersion.[21]

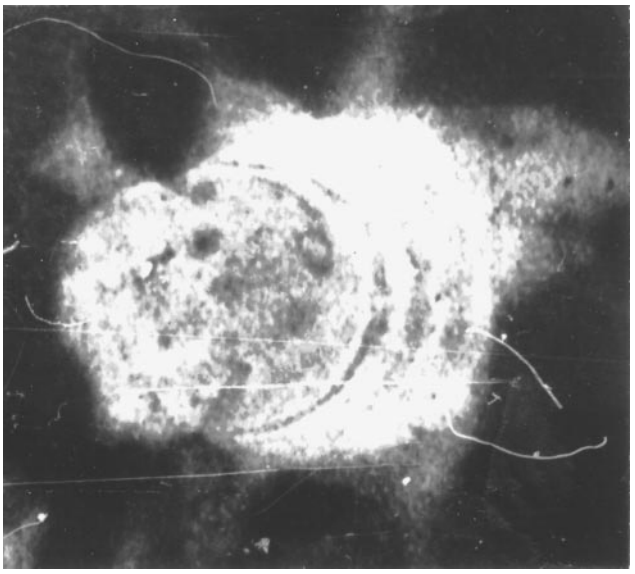

Fig. 2 A drop with steps in an iron oxyhydroxide dispersion.[21]

classical work:[21] 'In conclusion, one should note another surprising analogy. The affinity between the birefringent sols and liquid crystals (mesomorphic substances, according to Friedel) is so big, that, under a superficial consideration, one can be taken for another. This is even more amazing, since two kinds of these sols correspond to the two main types of mesomorphic substances, studied by Friedel. The first, nematic type, has the structure with the long axes of its molecules situated parallel to each other. The second, smectic type, has the structure, where molecules are not only parallel, but are separated by equal distances in the direction of their long axes. The analogue to the first type is the structure of V_2O_5, the analogue to the second is the structure of FeOOH'.

The same point of view was expressed by Zöcher later, in 1954, in his special work 'Tactosols and Mesophases'.[26] He supposed that tactosols were similar to mesophases only phenomenologically, while microscopically these two classes of compounds were absolutely different. Thus, 'these both kinds of anisotropic media were, indeed, totally different' (ref. 26, p. 85).

‡Tactoids were found for a series of inorganic sols, such as benzopurpuryne 4B and chryzophenine,[21] and also for water solutions of the tobacco mosaic virus.[25]

Only towards the end of the 1960s did Zöcher realise[27,28] the necessity to recognise the actual identity of anisotropic inorganic sols and liquid crystals. However, he had classified these sols separately, and called them 'phases of a higher order' or 'superphases'. The reasons for this, according to Zöcher, were not only the much larger size of structural units in sols, but also the different nature of forces acting between the sol particles. In classical thermotropic liquid crystals, dispersion and repulsion forces prevail, while in superphases the forces of electrical ions (present in water) play a considerable role together with dispersive interactions.

Nevertheless, superphases, according to Zöcher, should be attributed, with certain reservations, to liquid crystals. These are his exact words: 'Due to the close analogy, it is, probably, inevitable to include nematic and smectic superphases into the domain of liquid crystals. Nevertheless, the physico-chemical nature of superphases strongly differs from the nature of low-molecular organic substances, having the mesophases. The latter can be obtained by changing the temperature and concentration, the former—only by changing the concentration'.[27]

In fact, as we will see later, the influence of temperature on the phase behaviour of inorganic liquid crystals is not considerable. However, the thermal behaviour is not the main feature of mesophases. The principle feature is that both inorganic lyotropic superphases and classical thermotropic and lyotropic liquid crystals form, under certain conditions, thermodynamically stable phases, which exhibit long-range orientational order.

A boom in investigation and application of liquid crystals, which began in the 1960s, absolutely did not include the class of inorganic lyotropic mesophases. Until very recently they seemingly did not exist, they were absolutely forgotten. It is sufficient to say that there is not any, even the slightest, mention of inorganic lyotropic mesophases in numerous textbooks and monographs on liquid crystals. Only in the last few years has there appeared a certain interest in their properties. It was shown that not only the substances studied by Zöcher, but also some other dispersions of inorganic materials possessed a liquid-crystalline structure.

Consider now the properties of these mesophases in more detail. The currently known inorganic dispersions, in which the existence of mesophases has been proved, the mesophase types and areas of concentration, are shown in Table 1.

In addition to the substances summarised in Table 1, there is information about the existence of mesophases in water dispersions of some mineral clays, such as montmorillonite or bentonite and also in graphite acid and potassium phosphate.

Nematics

Vanadium pentoxide

We will start the description of nematics with the classic inorganic lyotropic liquid crystal—vanadium pentoxide. Its colloidal solutions have been studied in detail for many years, but not in connection with their liquid-crystalline properties.[29] It was shown that, depending on the V_2O_5 concentration, a colloidal solution exhibited the properties of either a sol or a gel. The concentration is usually determined by drying the samples at a temperature of 500 °C. For its expression, besides the usual chemical units, one commonly uses the number of water molecules n which correspond to one vanadium pentoxide molecule—$V_2O_5 \cdot nH_2O$.

The critical concentration, which corresponds to the transition from sol to gel, equals approximately 0.2 mol l^{-1} = 18 mass% = $V_2O_5 \cdot 250H_2O$. Below this concentration, a colloidal solution has the properties of a sol, above it has those of a gel.[30]

Methods used to obtain vanadium pentoxide sols and gels are extremely variable. Some of them can be utilised to obtain either one phase or the other.

Four main techniques are most commonly used. The first one is that originally elaborated by Biltz.[31] This involves preparation of a V_2O_5 dispersion in water. V_2O_5 is obtained by means of treatment of ammonium vanadate with hydrochloric acid. The obtained colloidal solution is called a Biltz sol. The second method is preparation of a dispersion of melted ammonium vanadate or vanadium pentoxide in water. The obtained solution is called a Müller sol.[32] The third technique is to let vanadium salt solutions pass through an ion-exchange column. As a result, decavanadium oxide is obtained. Then, this acid is decomposed in boiling water.[33] Sometimes, the fourth method of Prandtl and Hess[34] is utilised. This is the hydrolysis of the isoamyl ether of orthovanadium acid. This procedure allows one to obtain monodisperse sols.

X-Ray,[35–41] electron diffraction,[42,43] neutron diffraction,[40,44] and spectroscopic[45–48] studies together with electron microscopic observations[49–52] have shown that monocrystals in the form of small elongated solid particles, and/or of long flexible fibres or ribbons, depending on their formation conditions, may serve as the structural units in sols and gels of vanadium pentoxide.

The crystalline nature of these particles is clearly visible from the electron diffraction patterns (Fig. 3), obtained for the Biltz, Müller and ion-exchange sols.[42] These electron diffraction patterns coincide, in their main features, with the ones obtained from a solid V_2O_5 monocrystal.[35–37]

In most cases, freshly prepared V_2O_5 sols are optically isotropic. The particles of such sols are amorphous[45,53] and have a maximum size of 100 Å. However, the crystallisation process begins after several hours—monocrystals are being formed. These monocrystals continue to grow later. This phenomenon is called an 'ageing process'. Upon ageing, sol particles reach a critical size, which makes their orientational ordering possible. Then, birefringence appears, and different characteristic textures in the sample form (see below).

Sols age more rapidly under heating, or when an electrolyte (0.1 M NaCl, NH_4Cl, $CaCl_2$ or K_2SO_4) is added.[23] However, the main factor which influences the ageing process is increasing in the V_2O_5 concentration.[20]

The V_2O_5 sol ageing process was mainly studied either by optical[13,14] and electron[49–52] microscopy, or by X-ray methods.[30,35,36]

A freshly prepared Biltz sol (with a concentration of about 1 mass%) is practically monodisperse, with particles of length 20–40 nm. After one month, this sol becomes polydisperse, and the maximum length of its particles reaches 0.2–0.3 μm;

Table 1 Inorganic liquid crystals

Dispersion phase	Dispersion medium	Concentration/mass%	Type of mesophase
V_2O_5	H_2O	2–15	Nematic
AlOOH	H_2O	1.5–3	Nematic
$Li_2Mo_6Se_6$	CH_3CONH_2	4–10	Nematic
UO_2F_2	$CH_3COCH_3 + H_2O$	8–30	Nematic
$SiO_2 \cdot Al_2O_3 \cdot H_2O$ (imogolite)	$CH_3COOH + H_2O$	2–5	Cholesteric
FeOOH	H_2O	0.5–6	Smectic
H_2WO_4	H_2O	1	Smectic

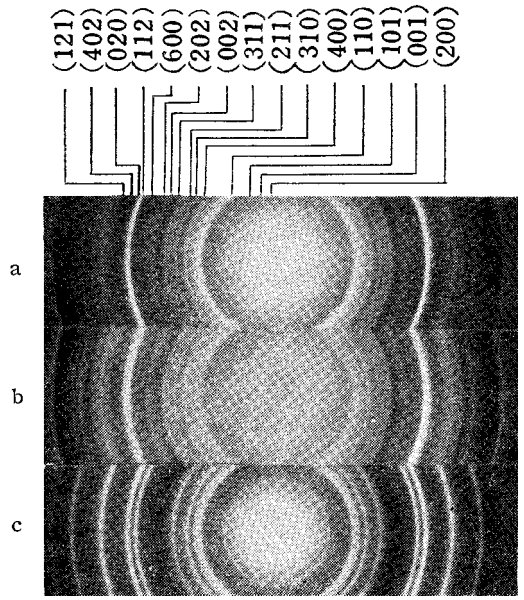

Fig. 3 Electron diffraction patterns for vanadium pentoxide obtained by the Biltz method (a), Müller's technique (b) and the ion-exchange method (c) (reproduced with permission from ref. 42).

after a further 4–6 months, it doubles; and after three years, the particle length is equal to 2.5–3.0 μm. However, the particle width remains practically constant and is equal to 14 nm.

The evolution of particles during the Biltz sol ageing process is clearly illustrated in Fig. 4, where micrographs obtained by means of an electron microscope[52] are shown. It is evident from this Figure that when the sol ages, the long flexible particles start to interweave, forming a net.

The old X-ray data,[35,36] however, give much smaller particle sizes (Table 2).

The particles in the freshly prepared Müller sol have the form of fibres with length 50 nm and width 15 nm. During the ageing process, they increase in size much more slowly than the particles in the Biltz sol. Thus, after one year, their average length is found to be approximately 0.4 μm, and after two years it is *ca.* 1 μm.[52]

Needle-shaped particles with a length of 1.2 μm, a width of 10–15 nm and a thickness of 1 nm are found in an ion-exchange sol.[30,52] They form conglomerates, the centres of which serve as the intersection points for sol particles (Fig. 5). The characteristic feature of this sol is that its particles do not increase in size when sol ages.

Finally, sols obtained by the Prandtl and Hess method (with a concentration of 0.1 mass%) contain rigid elongated particles with the following mean sizes: A = 150, B = 10 and C = 5 nm.[52]

Table 2 V_2O_5 particle sizes in the Biltz sol[35,36]

	Size/nm		
Ageing time	A	B	C
Freshly prepared	5	1	1
2 weeks	15	2	1
20 years	100	10	3

These sols possess a narrow particle-size distribution curve. Moreover, the particles in such sols probably remain unchanged during the course of the ageing process.

The data given above show that the Biltz sols are mostly subject to ageing. The longest particles are also found in these sols. This is probably due to the presence of ammonium ions (NH_4^+) in these sols. The NH_4^+ ions remain after V_2O_5 synthesis. Ammonium ions are not found in other sols. Indeed, as is well known,[23] the ageing process is accelerated considerably in the presence of salts of alkali metals and ammonium ions.

In the course of the ageing process, V_2O_5 particles increase their size mainly in one direction. This direction is determined by the specific character of the vanadium pentoxide crystal structure.

V_2O_5 monocrystals belong to the orthorhombic symmetry class. Their space symmetry group is *Pmmm*; the elementary cell parameters are: $a = 11.510$, $b = 4.369$ and $c = 3.563$ Å.[35–37] The V_2O_5 structure is constructed from trigonal bipyramids (Fig. 6). As is shown in the inset to Fig. 6, five points of each

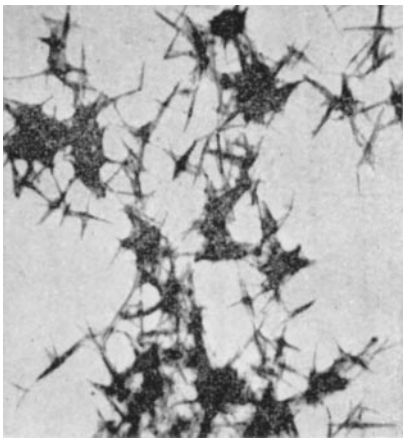

Fig. 5 Electron microscopy images of textures of ion-exchanged vanadium pentoxide. The sol is two months old. (Reproduced with permission from ref. 52.)

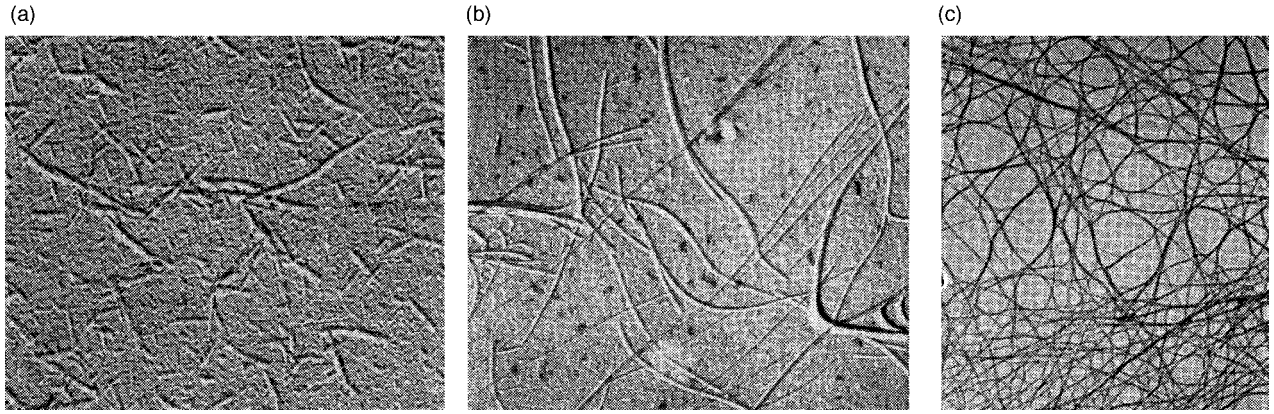

Fig. 4 Electron microscopy images of Biltz sol textures: (a) two days old; (b) two weeks old; (c) one year old (reproduced with permission from ref. 52).

such pyramid are occupied by oxygen atoms, and the pyramid centre is occupied by the vanadium atom.

The O(2) atom binds the two neighbouring pyramids so that they form a zigzag chain in the [001] direction. The chains are joined into layers, which are parallel to the (010) plane.

In the V_2O_5 sols and gels, the structure is divided into layers, which form the 2D structure of colloidal particles (Fig. 7). To compare this structure with that of a monocrystal, it is necessary to change the polar axis c to b. The 2D structure consists of mutually associated rhombic V_2O_5 blocks. Each of these blocks contains five V_2O_5 groups, *i.e.* two acute-angle VO_5 pyramids connected to similar VO_5 groups at the points. The block thickness, evaluated by means of X-ray[38–41] and neutron diffraction[40,44] experiments, is about 8.8 Å, which is in good agreement with the particle sizes (see above).

Now it is clear that when a sol is ageing, the V_2O_5 particles, in a 2D cell, grow preferably in the direction of the b axis and, to a smaller extent, in the direction of the a axis, while their thickness (the direction of the c axis) remains practically unchanged.

In a dispersion, the particles are bound by means of water molecules.[40,46] In the limiting case, when two molecular layers are bound by one water layer, the distance between the particles is 2.8 Å. With increasing concentration of water, the increasing number of water molecules in the layers leads to a stepwise increase of the distance between the V_2O_5 particles.

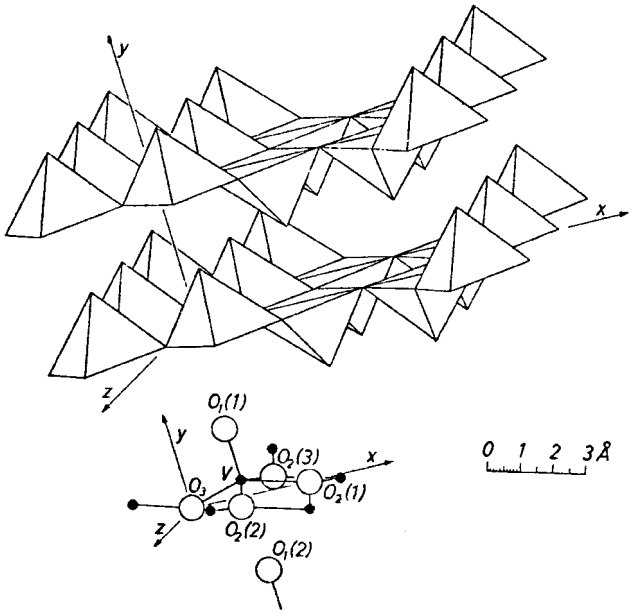

Fig. 6 Structure of crystalline vanadium pentoxide (reproduced with permission from ref. 37).

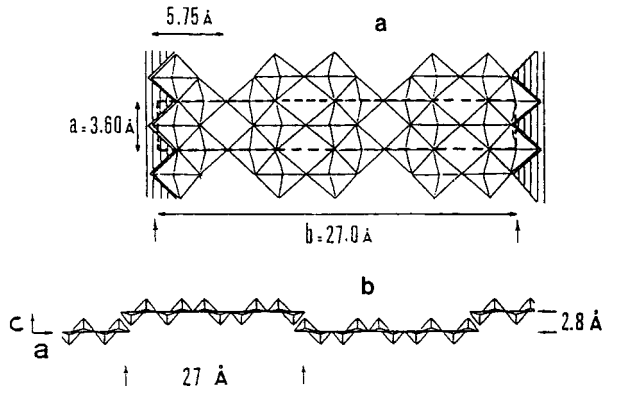

Fig. 7 Structure of a 2D vanadium pentoxide particle, projected onto the (001) (a) and (010) (b) planes (reprinted with permission from ref. 29. Copyright 1991 American Chemical Society).

The step is a multiple of 2.8 Å (Fig. 8). Thus, one can understand the process of sol formation, by considering the mechanism of V_2O_5 powder hydration.[44] The particles in the hydrated powder-like sample are compactly packed, and the distance between them is approximately 10 Å. This corresponds to $n \approx 2H_2O$. The particles have the same thickness but different widths. When a sample swells, the distance between the particles increases to 10–26 Å. Water penetrates only into cavities between the particles, which leads to their separation in the direction perpendicular to the layers. As the amount of water increases ($10 < n < 80$), the inter-particles distance increases to 50–250 Å. The latter circumstance allows the particles to rotate about their long axes. The ribbons may intertwine due to these multiple simultaneous rotations. Finally, in the region where $n = 250$–800 (a sol), the inter-particle distance equals 400–800 Å. This makes possible a free rotation of the particles around their long axes, without any interference from the neighbours.

As a whole, this model was confirmed by small-angle X-ray experiments.[38–41] The free, non-correlated motion of particles was observed for sols with $n = 5000$. However, beginning from $n \leqslant 600$, correlation in the positions of long axes was observed.

The existence of long-range orientational order in sols and gels of V_2O_5 was proved by optical microscopic and diffraction experiments. However, the character of the mesophase development was found to depend on the method of preparation of the colloidal solution.

In sols, obtained using the Biltz technique, as we have already mentioned, the process of mesophase formation is accompanied by tactoid growth (Fig. 1). This process has been studied in detail by means of polarised optical microscopy[54] and electron microscopy.[49] Tactoids are formed for V_2O_5 concentrations above some critical value, which depends upon the ionic force of the electrolyte present in the solution. The rate of tactoid formation increases with increasing V_2O_5 concentration. When the V_2O_5 concentration is constant, this rate increases with increasing electrolyte concentration.[54]

The structure of a tactoid is clearly visible in the electron micrograph shown in Fig. 9. It is obvious that the V_2O_5 particles are assembled in bunches. This helps the mutual orientation of particles.

The structure of tactoids (Fig. 10) may be imagined on the basis of the observations presented above and of the optical data. They typically have nematic organisation and may be considered as a nucleus of a nematic mesophase in a lyotropic solution. The spindle-like form of a tactoid means that the ratio between its surface tension and its viscosity is not very great.[54] In the course of the ageing process, the tactoid form

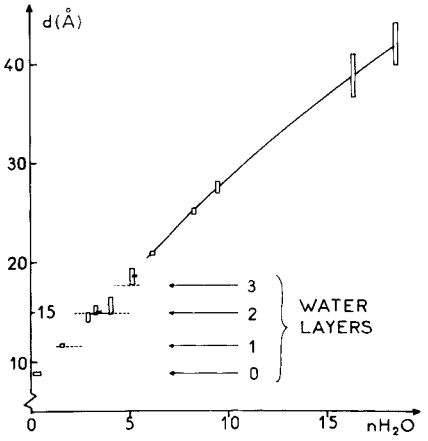

Fig. 8 Change of distance between the 2D layers in the process of water absorption by V_2O_5 (reproduced with permission from ref. 40).

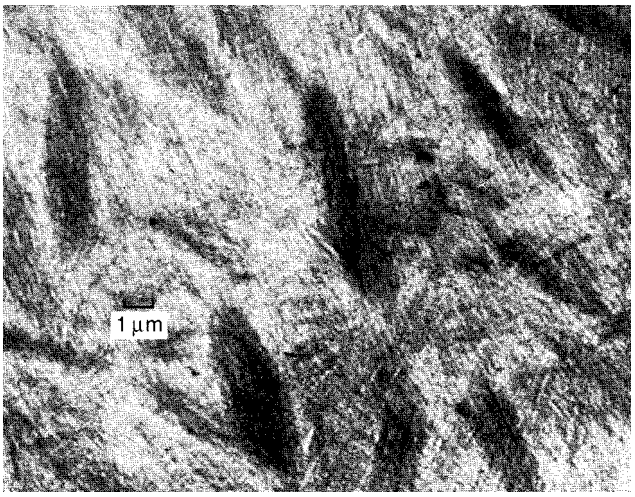

Fig. 9 Vanadium pentoxide tactoid (electron microscopy image) (reprinted with permission from J. H. Watson, W. Heller and W. Wojtowicz, *Science*, 1949, **109**, 274. Copyright 1949 American Association for the Advancement of Science. Readers may view, browse, and/or download this material for temporary copying purposes only, provided these uses are for noncommercial personal purposes. Except as provided by law, this material may not be further reproduced, distributed, transmitted, modified, adapted, performed, displayed, published or sold in whole or in part, without prior written permission from AAAS).

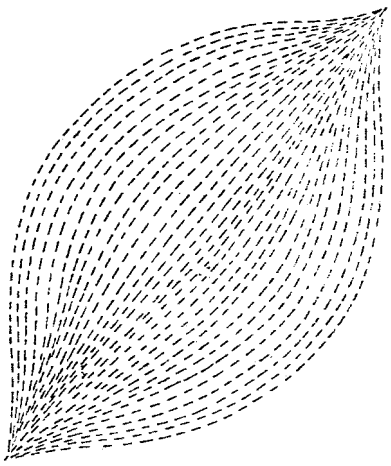

Fig. 10 Schematic arrangement of V_2O_5 particles inside a tactoid.[21]

sharpens, *i.e.* the elastic counteraction to the surface tension increases.

Tactoids exhibit strong positive dichroism. In the case when their long axes are parallel to the polarisation plane of the incident light they seem to be yellow, if long axes are perpendicular to this plane they are colourless.

V_2O_5 mesophases which have been aged for longer periods or have higher concentrations occupy practically the whole sample area. However, 'holes' of linear form, which reproduce precisely the tactoid shape, are observed in this sample (Fig. 11). These tactoids are called 'negative' or 'atactoids'. The space between such tactoids is filled with the dilute sol, which acquires induced birefringence when flowing. The conclusion has been drawn, on the basis of this fact, that the sol in the atactoid phase does not possess orientational order.[20] This has been proved by electron microscopy studies.[49] Fig. 12 shows an electron micrograph of a 72 h old sol, showing the atactoid phase. The values of the long axes and the relationships between them for tactoids and atactoids (Table 3) are found using micrographs analogous to that shown in Fig. 12. It is clear from these data that the long axes for tactoids and

Fig. 11 Vanadium pentoxide dispersion, containing atactoids.[21]

Fig. 12 Atactoid phase of a vanadium pentoxide dispersion (electron microscopy image) (reprinted with permission from J. H. Watson, W. Heller and W. Wojtowicz, *Science*, 1949, **109**, 274. Copyright 1949 American Association for the Advancement of Science. Readers may view, browse, and/or download this material for temporary copying purposes only, provided these uses are for noncommercial personal purposes. Except as provided by law, this material may not be further reproduced, distributed, transmitted, modified, adapted, performed, displayed, published or sold in whole or in part, without prior written permission from AAAS).

Table 3 Ratios between axes (a/b) and the long axis sizes (a) for tactoids and atactoids[49]

Type of phase	Number of measurements	a/b	a/μm
Tactoids	27	2.2–14.0	5.91–2.75
Atactoids	6	0.2–0.6	4.0–1.6

atactoids have quite similar values, while the ratios between the lengths of their long and short axes differ considerably.

Upon further ageing, the tactoid structure transforms into a discontinuous anisotropic mesophase, which shows fibrous structure under high magnification. These fibres have a transverse structure, clearly visible in Fig. 13. It consists of a number of alternating convexities and cavities with sizes of 65 and 35 Å, respectively. This structure corresponds to the actual arrangement of the V_2O_5 microcrystals. That is why the obtained picture is in accordance with the presence of nematic ordering in this mesophase.

Magnetic and electric fields influence the tactoid structure.[20,55] Since V_2O_5 is paramagnetic, its particles are oriented in a magnetic field along the direction of the field. Tactoids are oriented in the same manner.

The influence of an electric field is more complex, since together with purely orientational effects, the particles are oriented by the flow. In ac fields (with a potential of 220 V), in the absence of a flow, the V_2O_5 particles are oriented perpendicular to the field. In dc fields (with a potential of 120 V) areas with particle orientations both perpendicular and parallel to the field are observed. The latter orientation is due to the flow.

In a dc field, tactoids are oriented by their long axes in the direction of the flow (along the field). They move parallel towards the anode, and are strongly deformed. Their head section is deformed into a sharp point (sometimes, into several sharp points), while their tail section becomes rounded. The polarised optical microscopy observations allow one to imagine the distribution of the V_2O_5 particles in such tactoids which is schematically shown in Fig. 14. Note that in the head part of the tactoid, where the flow is practically absent due to the narrowness of this area, the V_2O_5 particles are oriented perpendicular to the flow. All these data prove that dielectric anisotropy is negative in the nematic mesophase of V_2O_5.

Concluding this section, we will consider the influence of electrolytes upon the tactoids. The addition of small amounts (2–5 mmol) of NaCl and LiCl solutions leads to tactoid compression in the direction perpendicular to their long axes. Moreover, the addition of arsenic acid totally prevents the formation of tactoids. Since electrolytes strongly influence the tactoid mesophase, one can suppose that its formation in the

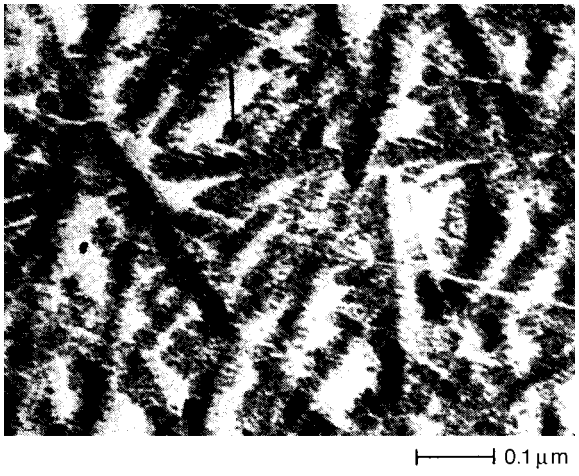

Fig. 13 Vanadium pentoxide dispersion: electron microscopy image, magnification × 120 000 (reprinted with permission from J. H. Watson, W. Heller and W. Wojtowicz, *Science*, 1949, **109**, 274. Copyright 1949 American Association for the Advancement of Science. Readers may view, browse, and/or download this material for temporary copying purposes only, provided these uses are for noncommercial personal purposes. Except as provided by law, this material may not be further reproduced, distributed, transmitted, modified, adapted, performed, displayed, published or sold in whole or in part, without prior written permission from AAAS).

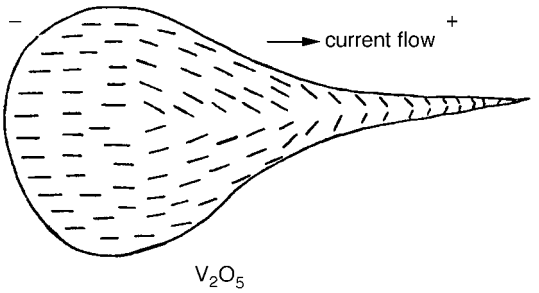

Fig. 14 Schematic arrangement of V_2O_5 particles inside a tactoid in an electric field.[20]

Biltz sols is connected, to a great extent, with the presence of a considerable number of ammonium ions.

However, in some cases, low-concentration Biltz sols give, in the course of the ageing process, immediately after formation of the isotropic solution, a discontinuous nematic phase (Fig. 15). Nevertheless, when this sol ages, tactoids form. This is possibly due to dividing of the sol into an isotropic phase and mesophase layers. This assumption seems to be credible, if one takes into account that the initial sol concentration is only slightly higher than the critical value, which is necessary for the formation of a mesophase.[56]

Sols and gels obtained by other methods do not form tactoid mesophases, but exhibit typical nematic textures. Sols and gels obtained by the ion-exchange technique are studied in detail in ref. 30. Sols with concentrations lower than 0.12 mol l^{-1} = $V_2O_5 \cdot 500H_2O$ are optically isotropic; however, for higher concentrations both sols (0.17 mol l^{-1} = $V_2O_5 \cdot 350H_2O$) and gels (0.85 mol l^{-1} = $V_2O_5 \cdot 65H_2O$) give typical nematic textures (Fig. 16). A nematic mesophase also appears when a gel is diluted with toluene. The addition of NaCl electrolyte rapidly leads to suspension flocculation. The appearance of textures remains unchanged when the sample is heated to 80 °C and also under the action of a magnetic field (1.7 T) and an ac electric field (10^6 V m^{-1}, f = 100 kHz). However, both sol and gel can be easily oriented by shifting the upper cell glass.

Birefringence in a gel sample was measured at a concentration of 0.3 mol l^{-1}. It was found to be equal to 10^{-2}, which was in good agreement with values for other lyotropic nematics.[57]

A small-angle X-ray experiment gives a diffuse reflection typical for mesophases in capillaries with radial director orientation. It has been found from the X-ray data that the mean distance between the ribbons is about 160 Å. Thus, we do not possess much information on the original lyotropic liquid crystal, vanadium pentoxide, which seems to be quite well studied. We know only its type of superstructure (nematic), the organisation of its structural units, the absence of orientation in magnetic fields and athermal behaviour.

Aluminium oxyhydroxide

Aluminium oxyhydroxide sol was obtained by Zöcher and Torok[24] by dissolving aluminium foil in acetic acid in the presence of a small amount of mercury acetate. After boiling, the cooled studied solution became opaque and a strongly birefringent gel was formed. The addition of water during the boiling process transformed this gel into a sol. The latter exhibited birefringence only when flowing. However, the birefringence dispersion obtained from this sol was retained for quite a long time.

The Zöcher sols and gels contain some acetic acid, which can not be removed by boiling. Its presence has a considerable effect on the optical properties of the obtained sol (see below).

A more recent method of preparation of the AlOOH sols and gels is the hydrolysis of isopropoxyaluminium in the presence of HCl and NH_3 (aq).[58] The properties of the

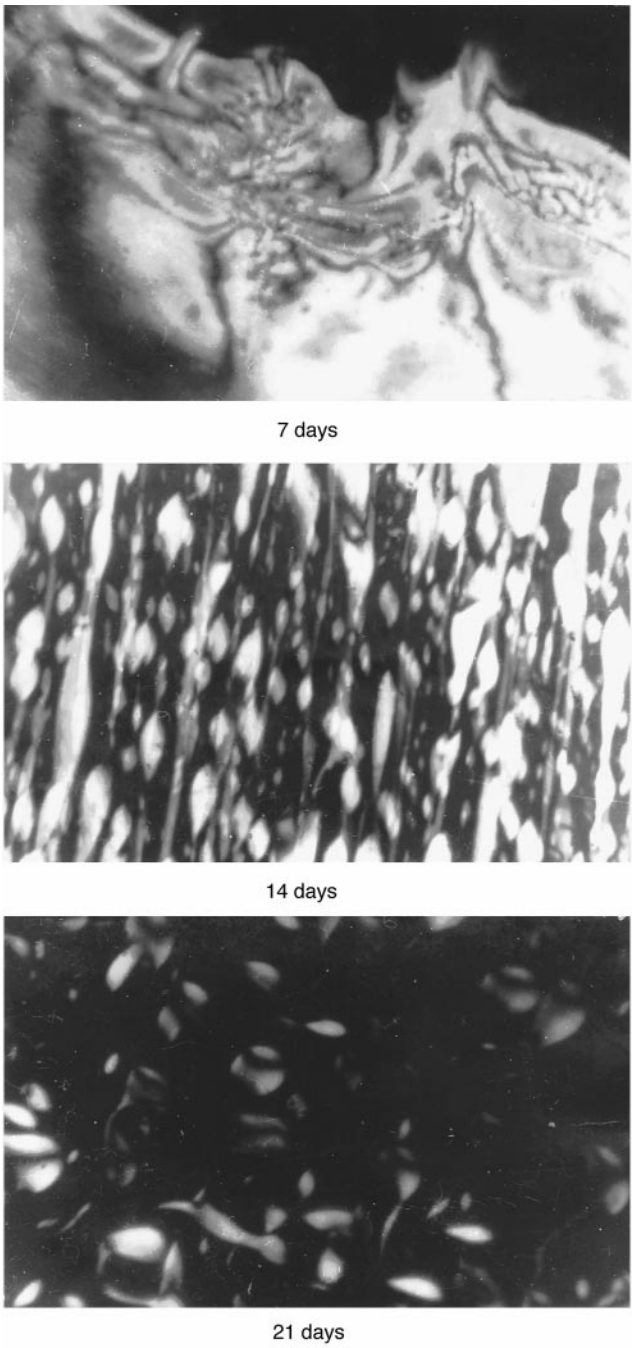

Fig. 15 Vanadium pentoxide dispersion with a concentration of about 1 mass%. The texture change in the course of the ageing process.[56]

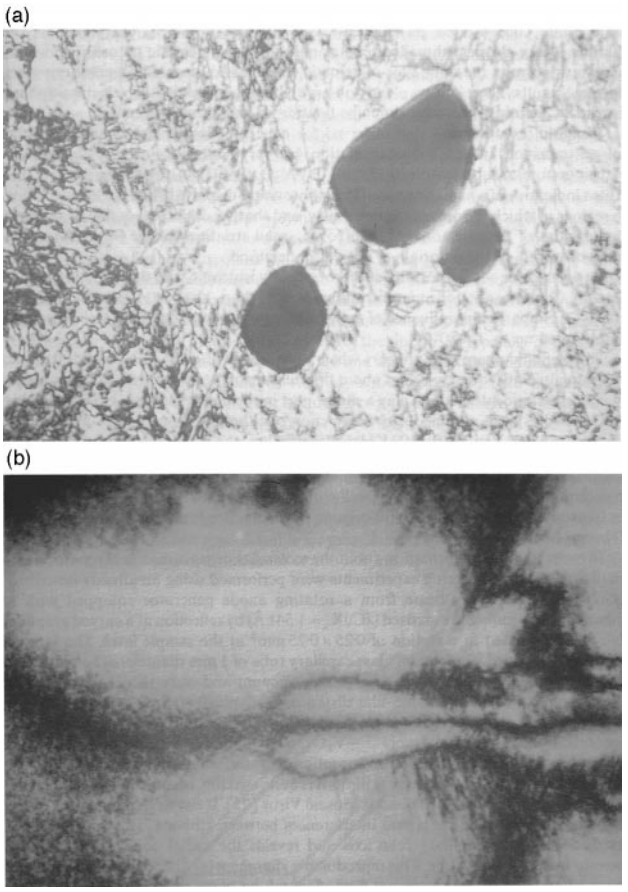

Fig. 16 Textures of a vanadium pentoxide dispersion: (a) gel, concentration 0.85 mol l^{-1}; (b) sol, concentration 0.17 mol l^{-1} (reproduced with permission from ref. 30, Taylor and Francis).

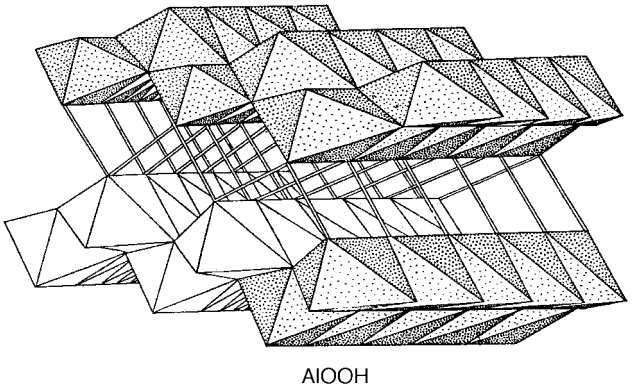

Fig. 17 Boehmite lattice: octahedral layers connected by hydrogen bonds.[62]

obtained dispersions also depend, in this case, upon the quantity of HCl and NH_3 (aq) participating in the reaction.

X-Ray,[58,59] electron diffraction[60,61] and electron microscopy[58] investigations have showed that the structural units of aluminium oxyhydroxide are γ-AlOOH (boehmite) crystals.

Boehmite belongs to the lepidocrocite structural type (Fig. 17). This is a rhombic structure of the *Cmcm* space group and with the following unit cell parameters: $a=2.86$, $b=12.2$, $c=3.69$ Å.[62–65] The aluminium ions lie in the centres of octahedra. Each such ion is surrounded by five oxygen ions and one OH ion. The layers of octahedra are connected to one another by hydrogen bonds. It is most probable that the hydrogen bonds are broken in dispersions, so the dispersion phase consists of ribbon-like particles. The thickness of any of these ribbons is equal to the thickness of the bemite layer.

Similarly to vanadium pentoxide, the aluminium oxyhydroxide mesophase forms tactoids when it is stored for a long time.[24] Fig. 18 shows micrographs of tactoids obtained in polarised light with different angles of rotation of the polarisation plane with respect to the main axis of a tactoid. These conoscopic pictures agree well with the model of the nematic arrangement of the AlOOH particles in a tactoid (see Fig. 10).

Aluminium oxyhydroxide tactoids exhibit slight positive birefringence.[66] After some time, tactoids join together forming a large mesophase region, containing sometimes atactoid inclusions. These mesophase areas have typical *schlieren* textures with clearly visible disclinations (Fig. 19).

The tactoids, which contain a minimal amount of acetic acid remnant, show an interesting stripe structure.[67] This structure is oriented perpendicular to the long axis of the tactoids (Fig. 20). The tactoid edges look jagged. As a rule, the distance between the neighbouring 'teeth' is about 3–6 μm.

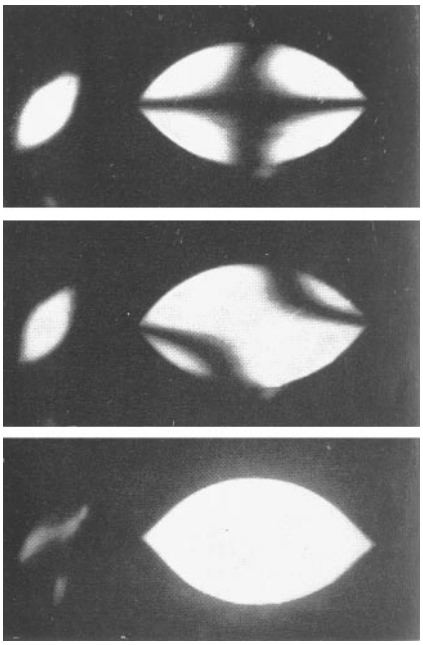

Fig. 18 Aluminium oxyhydroxide tactoids. The angle between the microscope nicols: 90° (top); 10° (middle) and 45° (bottom). (Reproduced with permission from ref. 24.)

Fig. 19 *Schlieren* texture of aluminium oxyhydroxide (reproduced with permission from ref. 66).

Separate layers of the transverse-stripe structure exhibit negative birefringence. This is clearly visible if the stripe structure is placed parallel to the sample plane. When two such tactoids merge together, a network of layers may be formed.

Separate elements of the transverse-stripe structure have the form of tactoids with dimensions 20×30 μm.

In this connection, the assumption has been made[67] that these tactoids are formed by two kinds of particles, which are needle-like and thread-like. These particles are placed perpendicular one to another and exhibit birefringence of different signs.

If a 1 M solution of acetic acid is added to this tactosol, the stripe texture disappears, and the tactoids return to their initial form.[67]

If a low-strength dc electric field is applied, the tactosol is displaced towards the cathode (the sol is charged positively). Then, in the cathode area, the pH increases and the aluminium oxyhydroxide concentration also increases. The transverse-stripe tactoids exhibit similar behaviour, but the stripe texture disappears and tactoids acquire positive birefringence.

There are still no data on the mesomorphic structure of AlOOH gels; however, it is known to form easily ordered structures.[58,60]

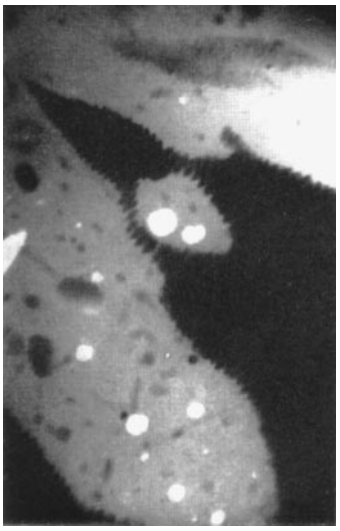

Fig. 20 Aluminium oxyhydroxide tactoid with 'teeth' (reproduced with permission from ref. 67).

Lithium molybdenoselenite

Lithium molybdenoselenite, $Li_2Mo_6Se_6$, is a member of a whole class of compounds having the general formula $M_2Mo_6X_6$, where X = Se, Te and M = Li, Na, K, Rb, Cs, In, Ag, Cu.[68,69] These substances are now intensively studied, since some of them appear to be superconductors.

Lithium molybdenoselenite is synthesised from $In_2Mo_6Se_6$ by a displacement reaction in the presence of lithium iodide.[70] Indium molybdenoselenite is obtained from its elements by means of direct synthesis at 1050 °C.

The isomorphic compounds $M_2Mo_6Se_6$ exhibit a hexagonal symmetry with $P6_3/m$ space group. They have a quite peculiar structure,[68,69] constructed from $(Mo_3Se_3)_\infty$ chains, formed on the basis of (Mo_6Se_6) icosahedra, which, in their turn, appear to be two (Mo_6 and Se_6) interpenetrating octahedra (Fig. 21). The (Mo_6Se_6) chains lie along the [001] axis as is shown in Fig. 21(b). Thus, each such chain may be considered as a quasi-one-dimensional structure.

It has been shown[71] that some compounds of the $M_2Mo_6Se_6$ class can be dissolved in highly polar solvents, such as dimethyl sulfoxide and *N*-methylformamide. This produces gels, which can be further diluted by the same or a less polar solvent, such as acetonitrile, glycerol and methanol. However, the obtained sols and gels are not stable. After 3–4 weeks from their formation, flocculation takes place and a flake-like insoluble residue is deposited.

Electron microscopy studies of lithium molybdenoselenite[71] show that the stick-like crystalline particles with lengths of the order of 2 μm serve as the structural unit for the dispersion. These particles represent, probably, separate chains surrounded by hydrated lithium ions. Electron microscopy also reveals a tendency of the $Li_2Mo_6Se_6$ crystals to orient themselves in one direction (Fig. 22).

In a narrow concentration range, between 4 and 10 mass%, the $Li_2Mo_6Se_6$ dispersion in *N*-methylformamide exhibits a structure[72] typical of nematic liquid crystals (Fig. 23). An analogous texture is observed when adding, in the ratio 1:3, acetonitrile into the *N*-methylformamide solution. The obtained nematic structure is destroyed with time (from several hours to several months). It breaks into separate anisotropic and isotropic areas.

X-Ray investigations[72] show the presence of a large variation in the particles size—from 10 to 1000 Å. The evaluation of the particle diameter allows one to assume that the chains are isolated and spontaneously oriented in one direction. Thus, a nematic type of ordering occurs in this case.

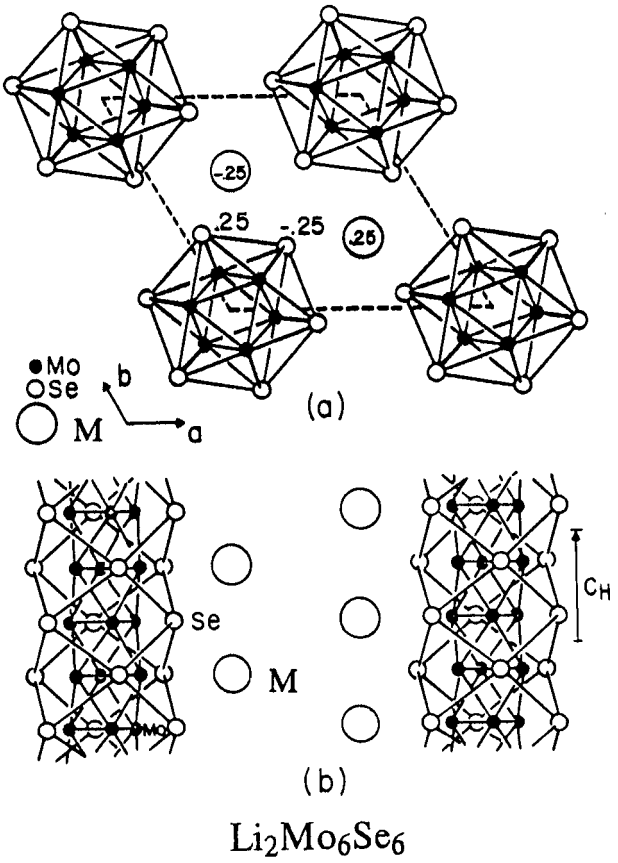

Fig. 21 $M_2Mo_6Se_6$ structure: (a) projection onto the *ab* plane; (b) projection onto the *ac* plane (reproduced with permission from ref. 68).

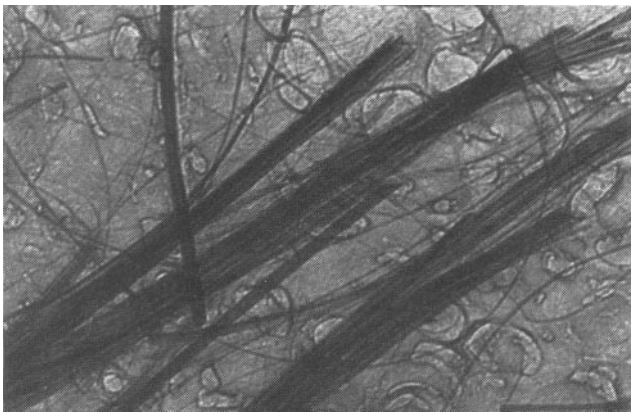

Fig. 22 Texture of a lithium molybdenoselenite gel (electron microscopy image) (reproduced with permission from ref. 71).

Although the physical properties of the nematic phase of lithium molybdenoselenite have not yet been studied, one may suppose that this case is the first example of the manifestation of orientational ordering in a system of current-conductive particles. This promises interesting peculiarities in the behaviour of this nematic.

Uranyl fluoride

Uranyl fluoride was prepared by means of the dissolution of uranium(III) oxide in a stoichiometric volume of plavic acid.[73] After multiple re-crystallisations, a water–acetone solution was prepared using heavy water. This solution was homogenised by heating to 40–50 °C. When acetone was added, the solution density was increased and light scattering occurred. When a certain acetone concentration was achieved, acetone was added into the heated UO_2F_2 water solution in small portions.

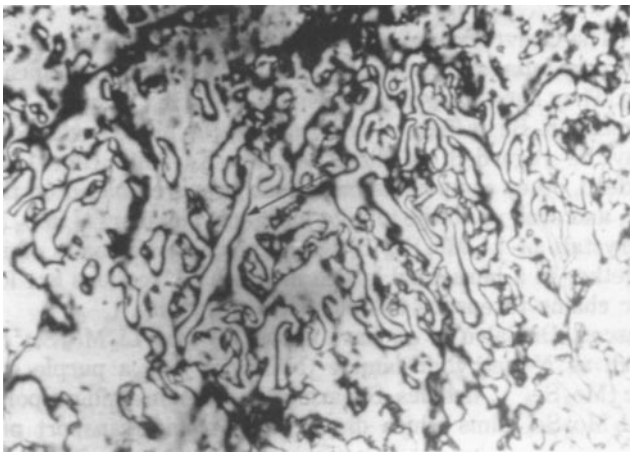

Fig. 23 *Schlieren* texture of lithium molybdenoselenite (reproduced with permission from ref. 72).

Orientational ordering typical of a nematic mesophase was discovered in such a solution by studying the NMR spectrum of the acetone protons[74] (Fig. 24).

Our microscopy investigations have confirmed the formation of a nematic mesophase in this case. A typical texture of the water–acetone UO_2F_2 solution, obtained by the edge-drying method, is shown in Fig. 25.

A detailed study of the NMR spectra[73,75] allows one to determine the temperature and concentration ranges where the mesophase is present. Fig. 26 shows the dependence of the temperature range of the existence of the nematic mesophase upon uranyl fluoride concentration, for different concentration ratios between acetone and D_2O. The nematic mesophase region occupies an intermediate area between the isotropic phase and the frozen solution. When the UO_2F_2 concentration diminishes, this area becomes narrower due to lowering of the

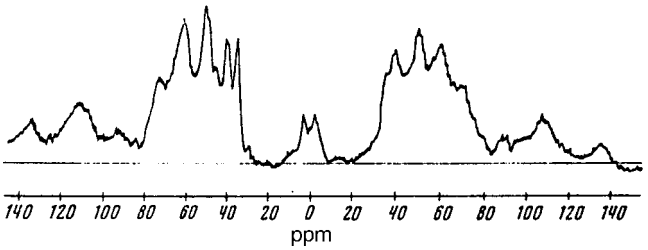

Fig. 24 NMR spectrum of the acetone protons in the uranyl fluoride–acetone–water system at $T = 4$ °C (reproduced with permission from ref. 73).

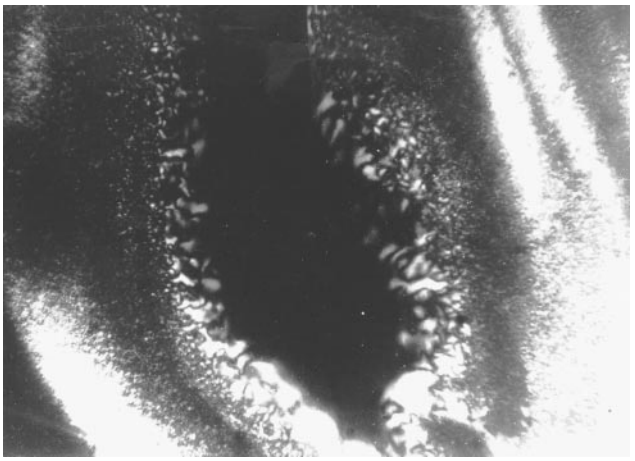

Fig. 25 Texture of the uranyl fluoride–acetone–water system (edge-drying method).

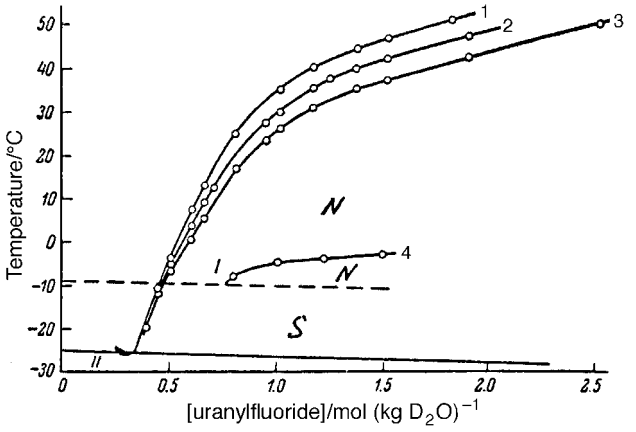

Fig. 26 Change of the temperature area of the existence of the nematic mesophase with changing uranyl fluoride concentration. Concentration of acetone: (1) 18.5; (2) 15.5; (3) 12.0; (4) 5.0 mol (kg D_2O)$^{-1}$. (Reproduced with permission from ref. 75.)

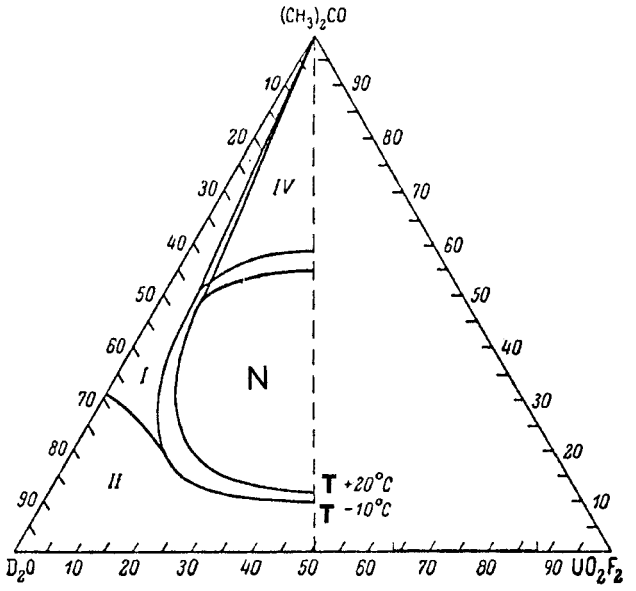

Fig. 27 Phase diagram of the uranyl fluoride–acetone–water system: (I) isotropic phase; (II) frozen solution area; (III) nematic mesophase; (IV) phase separation area. (Reproduced with permission from ref. 75.)

temperature of the nematic–isotropic liquid phase transition. For UO_2F_2 concentrations lower than 0.30 mol (kg D_2O)$^{-1}$ [for an acetone concentration in the system lower than 12–18 mol (kg D_2O)$^{-1}$] the nematic phase is no longer observed. Decreasing the acetone concentration in the system leads to narrowing of the temperature range of existence of the nematic mesophase.

Studies of this system in the region of high acetone concentrations [*ca.* 28–40 mol (kg D_2O)$^{-1}$] allow one to assume[75] the existence of another liquid crystalline mesophase in this region. This phase was characterised by an NMR signal typical for lamellar or hexagonal mesophases. However, detailed studies of this mesophase have not been carried out.

Fig. 27 represents the phase diagram of the system studied. It is clear from this figure, that at $T = -10\,^{\circ}C$ the nematic phase occupies a central part of the diagram, which lies between the isotropic phase and the frozen solution (II). As the temperature increases, the mesophase area becomes narrower, while the isotropic phase area widens. Unfortunately, it was not possible to investigate, by means of the NMR method, a mesophase lying in the area of high concentrations of uranyl fluoride.

The temperature and concentration dependences of the order parameter, S, for acetone in the nematic are obtained using the NMR technique.[73]

Fig. 28 shows such dependences, measured for different concentrations of uranyl fluoride and an acetone concentration of 12.0 mol (kg D_2O)$^{-1}$. It is clear that these dependences are characteristic of the nematic liquid crystals. The value of S in this case, however, is considerably smaller than that obtained for typical lyotropic nematics.[76] This is probably due to the fact that acetone is not included (or only partially included) within the structural units. According to ref. 73, the following dimer complexes serve as structural units for the mesophase considered:

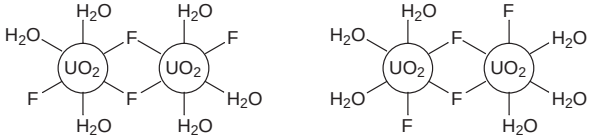

Their rigidity is ensured by the bridges consisting of fluorine atoms of two kinds, which connect the two uranyl fluoride molecules. If this assumption is correct, then it will be easy to explain the low values of S. Indeed, the acetone molecules follow only sterically the nematic ordering of dimers.

Further studies of ^2H and ^{17}O NMR spectra of water molecules introduced into such a system as a small-weight additive, allowed the detection[77] of quadruple splitting (typical for nematics) for a whole range of uranyl fluoride-containing lyotropic compounds. Heavy and normal water, tributylphosphate and benzene were investigated as dispersion systems. In addition, analogous splittings were found in systems containing tributylphosphate and uranyl nitrate, perchlorate, sulfate and chloride. However, no other proofs of the existence of liquid crystalline phases in these systems have been found. Nevertheless, the possibility of the existence of mesophases in solutions containing some actinoid coordination compounds is of fundamental importance.

Clays

Natural aluminosilicates (clays) are widely spread rock-forming minerals. They have a layered structure,[78,79] and, as a

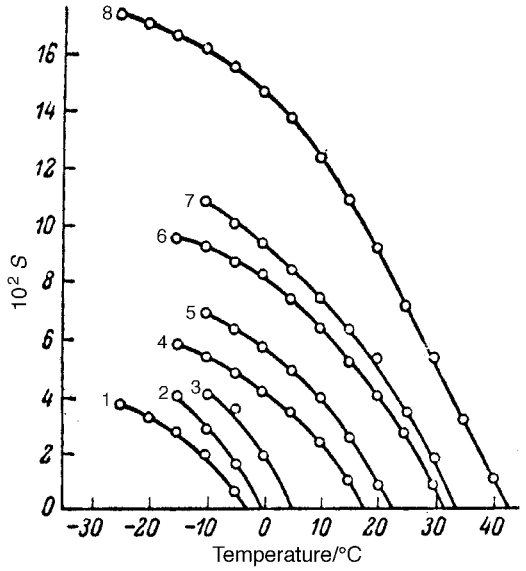

Fig. 28 Temperature dependence of the order parameter for the acetone molecules in the nematic mesophase of the uranyl fluoride–acetone–water system. The acetone concentration is 12.0 mol (kg D_2O)$^{-1}$. Uranyl fluoride concentrations: (1) 0.5; (2) 0.6; (3) 0.7; (4) 0.8; (5) 0.94; (6) 1.21; (7) 1.35; (8) 1.88 mol (kg D_2O)$^{-1}$. (Reproduced with permission from ref. 73.)

consequence, occur mainly in the form of finely dispersed powders, which are easily swollen in water. As a result, for some values of electrolyte concentration and pH, certain dispersive systems with liquid crystalline properties can be formed.

1. Imogolite. The dispersive particles of the clay mineral imogolite, $Al_2O_3 \cdot SiO_2 \cdot 2H_2O$, are thin pipes of diameter 25.2 Å, with the structure shown in Fig. 29.[80] The thickness of these pipes is equal to several thousand angstroms. The structure consists of gypsolite layers, in which the orthosilicate anion plays a connecting role. This anion occupies the vacant octahedral positions inside the gypsolite layer, separating the Si–OH hydrogen atom from three hydroxyl groups which surround each of these positions. Four Si—O bonds of this anion are from the layer, and they bind the protons into the SiOH structure. It is thus more correct to write the structural formula of imogolite as $(OH)_3Al_2O_3 \cdot SiOH$.

Imogolite gel was prepared[81] by means of dispersing the powder in an aqueous solution of acetic acid (pH = 3.5). This procedure was carried out in an ultrasound disperser and lasted 10 min. Then the obtained solution was centrifuged for one hour, until the total deposition of the insoluble matter. The upper part was evaporated off till its concentration became equal to 0.4 mass%. Then, acetic acid was added to the solution, till pH ≈ 3, and 0.02 mass% of NaN_3 was added as a stabiliser.

Polarisation optical microscopy observations have permitted the discovery[82] of a typical cholesteric 'fingerprint' texture (Fig. 30). This striped fingerprints structure disappears, as the weight ratio of imogolite in the dispersion increases (Fig. 31). This means that the helix pitch increases. A transition to the gel phase, which still has a cholesteric structure consisting of bent ribbons, takes place. The helix pitch p dependence is well described by the following empirical relation: $p = c^{-1.9}$, where c is the imogolite concentration.

In the high-concentration area (imogolite D), the dispersion is divided into three phases. The lower two of these three phases are cholesteric, while the upper one is isotropic. The phase behaviour and the helix pitch are not influenced by temperature.

A clearly distinguished layered structure with periods of 100, 15.6, 10, and 6.5 Å have been detected by means of electron microscopy studies. The last period is clearly visible in the micrograph shown in Fig. 32.

To explain the layered character of this structure, a theoretical model is proposed.[82] According to this model, the cholesteric mesophase consists of structural units in the form of layers ('rafts'). Each of these layers consists of four imogolite pipes. A schematic representation of this structure is shown in

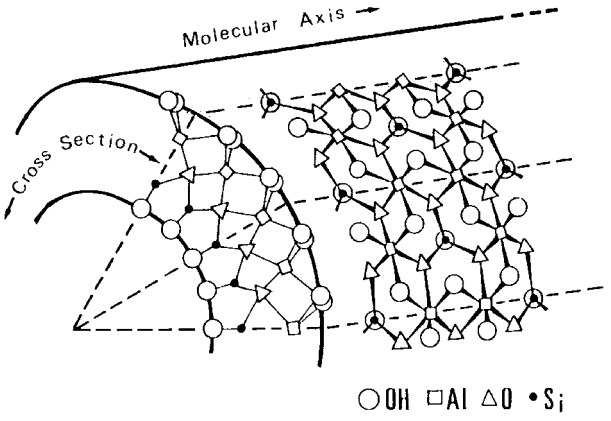

Fig. 29 Schematic view of a part of an imogolite pipe (reproduced with permission from ref. 80, Hüthig and Wepf Publishers, Zug, Switzerland).

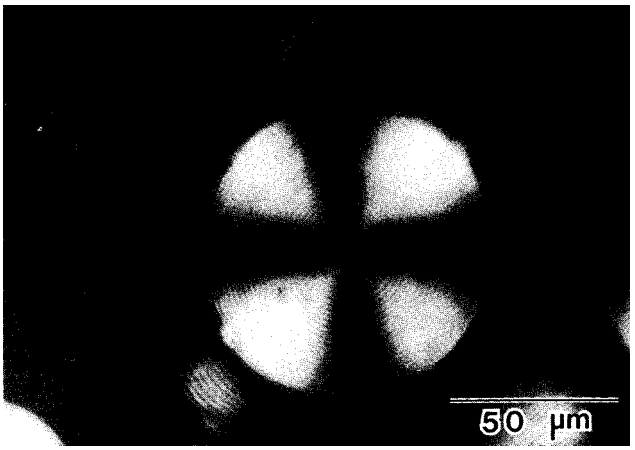

Fig. 30 A spherolite with a 'fingerprint' texture in the imogolite dispersion. The mass concentration is 0.0385. (Reproduced with permission from ref. 82, Hüthig and Wepf Publishers, Zug, Switzerland.)

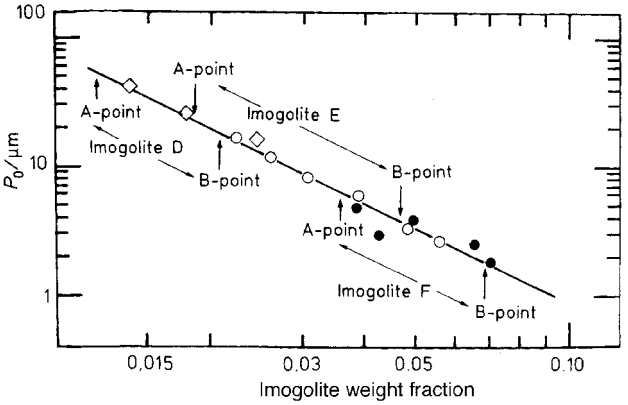

Fig. 31 Dependence of the helix pitch for the cholesteric mesophase of the imogolite–water–acetic acid system with changing concentration: the imogolites D, E and F are dispersion samples which differ in concentration (reproduced with permission from ref. 82, Hüthig and Wepf Publishers, Zug, Switzerland).

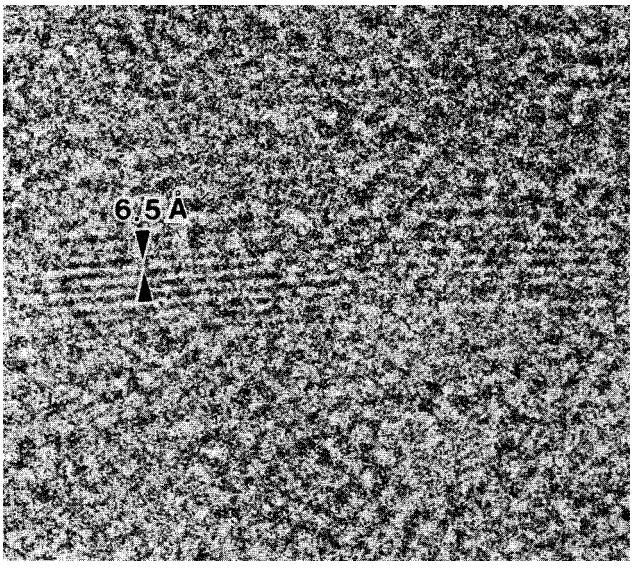

Fig. 32 Imogolite dispersion having a layered structure with a period of 6.5 Å (reproduced with permission from ref. 82, Hüthig and Wepf Publishers, Zug, Switzerland).

Fig. 33. It is easy to see that such packing of 'rafts' at an angle of 75° to one another, explains well the periodicity of the structure in the direction shown by the arrow. If the 'raft' packing is organised under an angle of 66.5°, then the layered structure will have a period equal (depending on the direction of observation) to 10 or 15.6 Å. The angle of 'raft' packing is determined by the imogolite concentration in the dispersion.

The described model assumes each 'raft' to be rotated by some small angle with respect to the neighbouring 'raft'. This leads to a cholesteric twist. According to ref. 82, the reason for this twist is connected to the mutual positioning of the end OH groups of the imogolite pipes. These groups are situated at the pipe surface in a spiral manner. The axes of these spirals coincide with the pipe molecular axes (Fig. 34). Thus, the imogolite structure is, indeed, chiral.

The imogolite mesophase was found to be a good model system to verify the application of the Onsager and Flory theories to the description of ordering in a system consisting of rigid rods.[81] It was shown that the phase behaviour of this dispersion agreed qualitatively with Onsager's predictions.

2. Montmorillonite. An aluminosilicate of the smectite group, montmorillonite, has a complex chemical organisation. The pyrophyllite unit $Al_2Si_4O_{10}(OH)_2$ with a partial replacement of Al^{3+} by Mg^{2+}, Fe^{2+} and Fe^{3+}, serves as the basis of the montmorillonite structure. Montmorillonite exhibits a layered organisation (Fig. 35), consisting of tetrahedra [SiO_4] and octahedra [$AlO_4(OH)_2$].[78,79] Alkali and alkaline-earth cations and water molecules can be found in the inter-layer space.

Montmorillonite easily absorbs water and electrolyte solutions, which are localised between the aluminosilicate layers. As a result, a gel is formed. It probably contains 2D montmorillonite layers as a dispersive phase.

A liquid crystalline mesophase was detected[83] in the montmorillonite gel. This gel was obtained as follows. The montmorillonite fraction containing particles with sizes of about 2 μm, was washed with 1 M sodium chloride solution, and freed later from chlorine ions by means of dialysis through a cellulose filter (pH = 7). Then, the solid sample was placed into a 0.03% sodium chloride solution. A swollen gel exhibited an anisotropic stripe texture, which darkened when the crossed nicols were rotating at 90°. The stripe direction lay at an angle of about 20° with respect to the maximal darkness direction, the width of the stripes was 2 μm and their length was 150 μm.

When the sodium chloride concentration is reduced, the stripes width also decreases. If, in these experiments, one uses montmorillonite particles with sizes less than 0.5 μm, then more regular and wider stripes will be observed.

If a surface active substance, *e.g.* cetyltrimethylammonium bromide, is added to the dispersion, then separate montmoril-

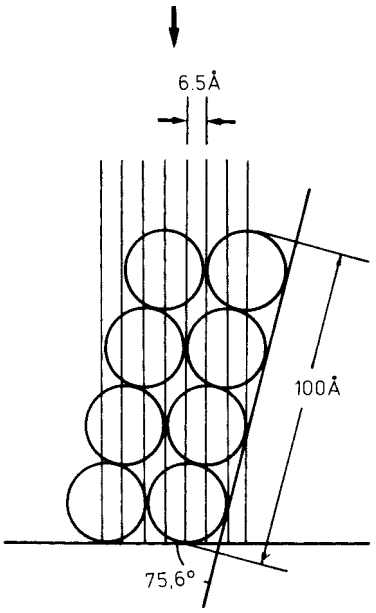

Fig. 33 Scheme of ordering of the structural units in the cholesteric mesophase of an imogolite dispersion (reproduced with permission from ref. 82, Hüthig and Wepf Publishers, Zug, Switzerland).

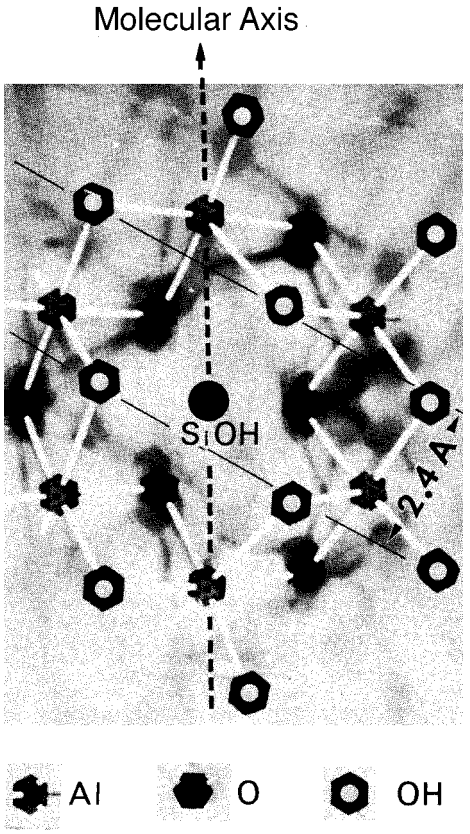

Fig. 34 Molecular model of the gibbsite unit of the imogolite pipe. The two continuous lines represent the OH group arrangement at 55° to the molecular axis, shown by the dashed line. The distance between the two lines is equal to 2.4 Å. (Reproduced with permission from ref. 82, Hüthig and Wepf Publishers, Zug, Switzerland.)

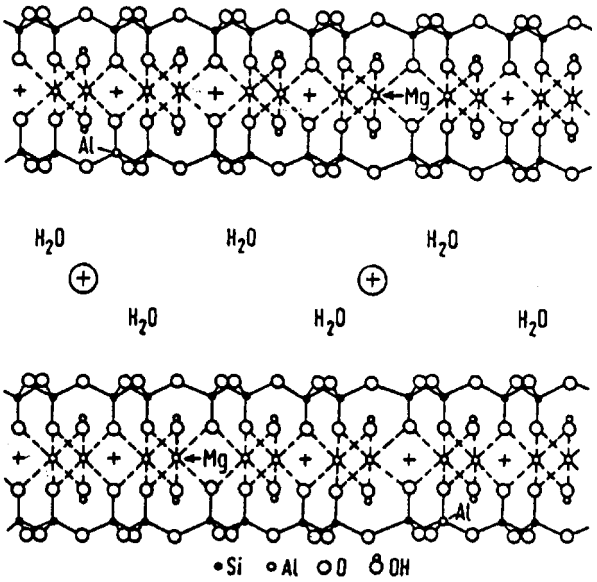

Fig. 35 Layered structure of montmorillonite. The positions of Al^{3+} ion substitution by Mg^{2+} and other ions are indicated. (Reproduced with permission from ref. 78.)

lonite small crystals, perpendicular to the stripe structure, will appear in the optical field. In this connection, it is natural to make the assumption that in the montmorillonite gel the particles are situated in the layers, which are parallel to the observed stripes. If this is true, then the montmorillonite gel should be classified as a smectic liquid crystal.

A bentonite dispersion, consisting of montmorillonite (79 mass%) with added quartz, calcite and gypsum, readily demonstrates birefringence when flowing. Areas of spontaneous optical anisotropy have been observed in concentrated dispersions.[83,84] This allows one to assume the existence of a mesophase in such a dispersion.

Smectics

Iron oxyhydroxide

We will start the consideration of smectics with the FeOOH sol. This is a true and well studied lyotropic liquid crystal.

The method of FeOOH synthesis has been elaborated by Zöcher and Heller.[85] It consisted of the slow hydrolysis of iron-(III) chloride at low temperatures, in the presence of ammonia solution. The hydrolysis lasted from 4 to 12 months. As a result, a dense, coloured residue was precipitated at the bottom of the reaction vessel. It was possible to use this residue directly for the investigations, or to centrifuge it until it became a paste which was then redissolved by heating for 3 weeks.

The FeOOH crystals serve as structural units for an isotropic gel (Fig. 36). Their sizes lie in the range from 50×400 to 140×700 nm. However, the issue of the FeOOH crystalline form is found to be quite difficult.

Indeed, iron oxyhydroxide exists in three modifications: rhombic α-FeOOH (getite), tetragonal β-FeOOH (acagapite) and rhombic γ-FeOOH (lepidocrite). X-Ray[86,87] and electron microscopy[88–90] investigations prove with no doubt that β-FeOOH crystals are present in sols obtained by means of the Zöcher method. However, earlier studies by Heller *et al.*[91] have shown that some complex processes in iron oxyhydroxide sols take place with time. In the beginning of the hydrolysis process, FeOCl is formed. It transforms gradually into β-FeOOH, and, later on, into α-FeOOH. Moreover, the time to the first transition is about 5–8 years, while that to the second ranges from several months up to 25 years.

Since the majority of researchers work with sols which have been aged for several years, then it becomes clear that β-FeOOH is present in these sols only as an intermediate form.

β-FeOOH crystals are tetragonal with unit cell parameters in: $a = b = 10.48$ Å, $c = 3.023$ Å space group $I4/m$.[86,87] The structure of β-FeOOH consists of a network of tetrahedra, composed of O atoms and OH groups, with Fe atoms lying in the centre of the tetrahedra. Water molecules are present in this structure; their removal leads to the transformation of FeOOH into α-Fe_2O_3 (Fig. 37).

If, to obtain a sol, one uses a concentrated solution of iron-(III) chloride, then, after 4–6 weeks, tactoids will be formed in the isotropic solution.[87,92] FeOOH tactoids are similar to those of V_2O_5 (Fig. 2). However, the former exhibit more pronounced circular form. Typical sizes of FeOOH tactoids are 0.2×0.1 mm.

However, low concentration Zöcher sols (1–6 mass%) with low pH ($\leqslant 1$), which are isotropic just after their preparation, can be, after some time, divided into layers. These sols form dense iridescent residues, which are called '*schiller*' (which means iridescent) layers.[20,21,27]

Optical microscopy allows one to observe typical smectic textures. Fig. 38(a) illustrates a step texture. The plane of this texture is perpendicular to the optical axis. Fig. 38(b) shows a texture in which the layers are oriented perpendicular to the figure plane. These textures demonstrate convincingly the layered smectic structure of the FeOOH sol.

The orientation of the particles with respect to the layers was studied by means of electron microscopy.[89] It was assumed that the particles formed layers, orienting their long axes in the layer plane. However, this structure was not in accordance with the observed optical properties—the direction of the optical axis and the positive birefringence. Recently, it was shown convincingly[90] that FeOOH particles were oriented with their long axes perpendicular to the layer plane, as is the case in typical smectics.

Calculations, realised with the help of the DLVO method, showed that the particles are packed inside the layers according to the quadric law, due to the existence of the second minimum in the potential curve. The distance between the particles was found to be approximately 300–400 Å.

There are two periods in the FeOOH smectic structure: the distance between the layers and the distance between the particles inside the layers. The inter-layer distance is of the order of magnitude of the wavelength of visible light. This leads to the clearly visible selective reflection in the homeotropic texture. The freshly prepared Müller layers look bright

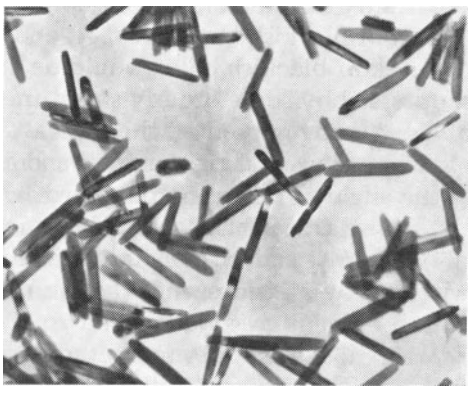

Fig. 36 Electron microscopy image of β-FeOOH crystals (reprinted from ref. 86: Y. Maeda and S. Hachisu, *Colloids Surf.*, 1983, **6**, 1, Copyright 1983, with permission from Elsevier Science).

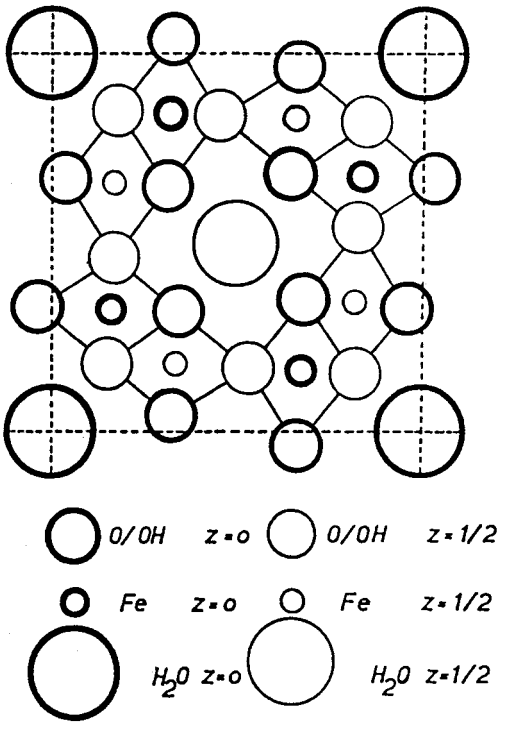

Fig. 37 β-FeOOH structure projected onto the (001) plane (reproduced with permission of the Mineralogical Society of Great Britain and Ireland).

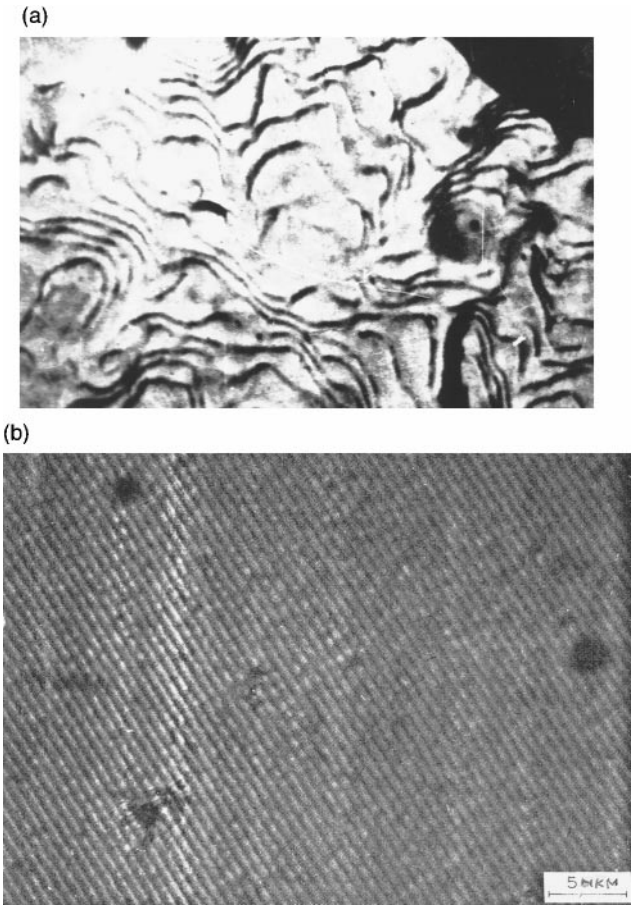

Fig. 38 Textures of the iron oxyhydroxide–water system: (a) step texture (reproduced with permission from ref. 27 reprinted from ref. 86: Y. Maeda and S. Hachisu, *Colloids Surf.*, 1983, **6**, 1, Copyright 1983, with permission from Elsevier Science); (b) layered texture.

green under normal illumination. When the light incidence angle is increased, they become sky-blue, green, blue and violet.[21] The schiller layers, lying perpendicular to the glass substrate surfaces, also exhibit selective reflection, if the FeOOH particle diameter has the order of magnitude of the wavelength of visible light.[90]

The inter-layer distance increases with time, which is proved by the change of colour from orange to red.[20] If the pH is increased from 1.5 to 3, the selective reflection wavelength is decreased twofold.[27] This phenomenon is accompanied by the appearance of strong dichroism: the layers look bright green under the initial light polarisation, and bright yellow, under light polarisation perpendicular to the initial light.[27]

An attempt was undertaken[93] to calculate the inter-layer distance for the homeotropic texture, using a simple interference formula. Data for sols of different concentrations (from 0.5 to 0.3 mass%) and of different ageing time (from 59 to 1695 days) were used. It was found that when a sol aged its inter-layer distance increased. With increasing concentration, the distance between layers could either increase or decrease. The mean inter-layer distance was found to be *ca.* 2000 Å. However, these estimations did not take into account changes in the particle sizes.

When a low electric voltage is applied, the sol is displaced towards the cathode. The selective reflection wavelength is simultaneously red-shifted.[21]

Magnetic fields do not influence the selective reflection; however, areas with negative birefringence parallel to the field lines appear.[21] This fact, together with the phenomenon of the rotation of the light polarisation plane (for incident light normal to the field lines), prove[92] that the sol particles are oriented by a magnetic field. Temperature has no effect on FeOOH sol behaviour.[20,21,27]

Table 4 Mean sizes of the particles in the dispersion phase of the tungstic acid–water[96]

Type	a/μm	b/μm	c/μm	$a:b:c$
A	11.7	4.05	0.15	100:35:1.3
B	14.6	5.0	0.35	100:34:2.4
D	2.27	0.75	0.044	100:33:1.95

Tungstic acid

Tungstic acid H_2WO_4 ($WO_3 \cdot H_2O$) is the second credible example of smectic mesophase formation. Its water dispersion is usually obtained as follows.[20] Sodium tungstate solution is treated with hydrochloric acid. The obtained fraction of solid particles is centrifuged and diluted with water to a low volume. The residue is centrifuged again and is diluted with water, thoroughly mixing the solution. The obtained mixture is then centrifuged several times. As a result, a residue is obtained which is dissolved in a large amount (*ca.* 200 cm^3) of water. Finally, an opaque dispersion, showing iridescent radiance when flowing, is obtained.

Microscopy[20,27] and electron microscopy[94–97] studies have shown that quite complicated particles form the dispersive phase. Just after the formation of the dispersion, one can observe elliptical particles with maximum sizes of 0.2–0.3 μm and their length and width increase rapidly with time. These are termed A-type particles [Fig. 39(A)] which possess low positive birefringence and are optically homogeneous. It is possible that these particles may be small tactoids, since the particle edges are not smooth, but jagged. These notches can serve as outlets for the smectic layers of real structural units.

As the considered dispersion ages, D-type particles are formed [Fig. 39(D)]. These are narrow crystals of absolutely perfect form. Comparison of the difractograms for D- and A-type particles shows that these objects are completely different in structure.

If the ageing time is short, then particles with intermediate forms will appear. These are referred to as B-type [Fig. 39(B)] and C-type [Fig. 39(C)] particles. The first of these types includes particles with plane-parallel ribs, but with elliptical ends. The second type includes eight-sided particles with straight ribs.

Particle size measurements give quite interesting results (see Table 4). In spite of large distribution of particle sizes, the ratio of particle dimensions is almost the same for each type, which proves the general nature of these particles.

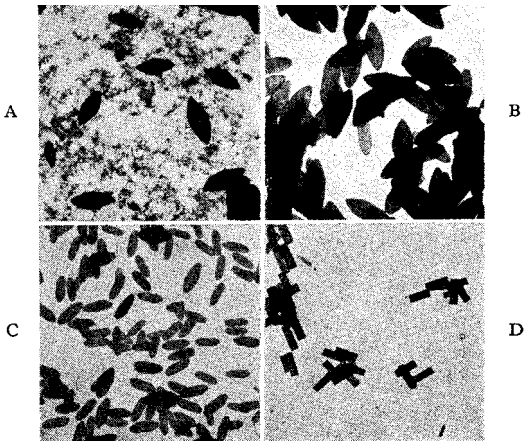

Fig. 39 Electron microscopy images of tungstic acid dispersion particles (reproduced with permission from ref. 94).

It is interesting that an isothermal transition between particles of different types is observed. The principal direction of this transition is A→B→C→D. However, a direct A→D transition is also observed. Since a considerable effect of the medium pH on these transitions is found, the assumption is made[95] that a change in the habitus of the tungstic acid particles is connected with a modification of their structure. This latter structural change is analogous to the transition: FeOCl→β-FeOOH→α-FeOOH (see above).

If the tungstic acid dispersion is stored for quite a long time, it will acquire the iridescent radiance characteristic of layered structures.[20] The smectic layers and the orientation of particles inside them are clearly visible in Fig. 40.

The inter-layer distance depends upon the concentration, pH and the presence of electrolytes in the solution.[20,27,98,99] Qualitative studies (by means of interference order observation) show that the inter-layer thickness increases with the degree of dilution. If the solution is diluted approximately 40-fold the distance between the layers increases approximately threefold. This is accompanied by an increase in pH of the solution.

Quantitative measurements were carried out by optical methods.[20,98,99] It was shown that the inter-layer distance decreased with increasing number of layers. Thus, in a sample containing 80 layers, the mean inter-layer distance was found to be 0.83 μm, while in a sample with 800 layers it was 0.65 μm.

The dielectric conductivity of the dispersive medium also influences the inter-layer distance. Using alcohol instead of water as the solute decreases this distance by a factor of 0.58.

However, the most considerable influence is caused by electrolytes. It is found[98,99] that different electrolytes with the same equivalent concentration, decrease the inter-layer distance to the same degree. If the electrolyte concentration is changed from 1×10^{-8} to 64×10^{-8} equiv. cm^{-3}, the inter-layer distance decreases from 0.9 to 0.2 mm.

All these facts prove the evident effect of electrostatic forces on the formation of such layers. An attempt has been made[99] to calculate the equilibrium distance between the layers, taking electrostatic and gravitation forces into account. The calculation scheme is similar to that of the DLVO method. Fig. 41 shows the obtained theoretical results together with the experimental data taken from refs. 98 and 99. It is clear that the calculated and experimental values of the inter-layer distances are in good agreement.

The above-described studies are, at the moment, the only ones on the smectic mesophase of tungstic acid.

Conclusion

The above-considered mesophases of inorganic substances represent most of the documented studies of lyotropic inorganic liquid crystals. In fact, there are many more such mesomorphic substances. However, the information on these mesophases is often contradictory and, hence, needs careful verification. As an example, one may consider the reports on the observation of mesophases in the so-called graphite oxide[100–102] and in calcium phosphate.[103]

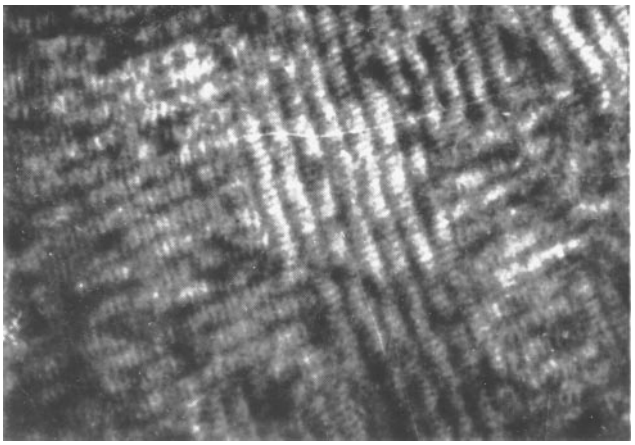

Fig. 40 Smectic texture of the tungstic acid (reproduced with permission from ref. 27).

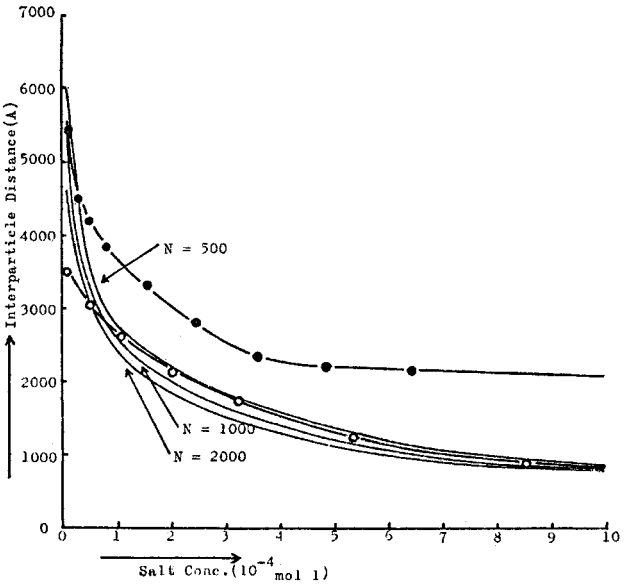

Fig. 41 Dependence of the inter-layer distance in the smectic phase of tungstic acid upon the electrolyte concentration: the solid points represent the experimental data of ref. 99; the open points show the experimental results of ref. 99; the continuous lines indicate the theoretical estimations of refs. 98 and 99 (reproduced with permission from ref. 98).

In this connection, one needs to point attention to the old work of our compatriot P. P. von Veimarn.[104,105] He obtained anisotropic dispersions of such simple ion salts as barium sulfate, calcium chloride, *etc.*

Lyotropic mesophases, as we see, are formed by inorganic compounds which are very different in their chemical nature. However, they all have similar structures: layered or island-like, *i.e.* structures composed of separate elements of considerable sizes. Examples of layered structures are vanadium pentoxide, aluminium oxyhydroxide, imogolite, montmorillonite and other clays. An example of and island structure is lithium molybdenoselenite, which consists of long columns.

When interacting with a solvent, such structures are easily decomposed into separate fragments (layers or columns), which become anisometric structural units of the forming mesophases.

Such a scenario of the formation of the lyotropic mesophases does not exclude an alternative process, whereby mesophases may appear due to the ordered arrangement of the bulk anisometric crystals. This latter scenario is, probably, realised in the cases of iron oxyhydroxide and tungstic acid. At the moment, the situation with the uranyl fluoride dispersion is unclear; the structural unit in the form of the molecular dimer seems to be improbable for formation of the colloidal solution.

The second peculiarity of inorganic liquid crystals is that they exhibit only one mesophase. This is probably a consequence of the large sizes of their structural units. Indeed, the reorganisation of such large structural elements requires considerable energy. However, as we have observed in the cases of aluminium oxyhydroxide and uranyl fluoride, there are some facts that can be interpreted in favour of the existence of highly ordered mesophases. It remains unclear, in this connection, why the studied gels and sols possess only one and the same mesophase. All these facts should be thoroughly studied.

The third characteristic feature, the narrow concentration interval of the existence of mesophases and their athermal behaviour, are the consequences of the large sizes of the structural units.

And, finally, the fourth peculiarity: the influence of electrolytes. This last characteristic feature makes inorganic mesophases similar to organic micellar and chromic liquid crystals.

If we now consider the fact of the existence of inorganic lyotropic mesophases, taking into account all the above-described peculiarities, it is necessary to point out that the appearance of orientational ordering is a quite widespread form of organisation of both organic and inorganic solutions. While organic mesophases have been studied in detail, inorganic liquid crystals still wait for their turn. Unfortunately, one can say that, since they have been neglected for so long, we deal now with a quite new and unexplored area.

By this statement, I mean the following. Considerable experimental material, concerning mainly the fact of the existence of mesophases in inorganic lyotropic systems, has been collected thus far. In some cases, there are even structural proofs of mesomorphism. However, most attention has been paid to the similarity between these mesophases and the well studied organic liquid crystals. There are differences, which are most interesting, since they are determined by the specific character of the inorganic mesophases. After all, these differences are due to the unequal sizes of the structural units in these two systems. One can say that the structural unit sizes in inorganic lyotropic systems are one order of magnitude greater than in organic lyomesophases. The elastic behaviour in these former systems is completely unknown. Here we will probably deal with, already discussed theoretically,[106] but not observed experimentally, second-order elasticity: when not only the structural units, as a whole, but also their constituent parts will participate in bending deformations.

The issue of elasticity is only one of many physicochemical problems concerning inorganic lyotropic liquid crystals. The other, which is closely connected with this former: is the Fredericks transitions. Here one should also expect some serious differences connected with the greater (than in the well studied mesophases) structural unit sizes.

Finally, the phase transitions in the above-described systems are athermal. However, the concentration areas of phase stability are known, but they have not yet been studied in detail.

All these unsolved problems, together with the issues of electric and magnetic field effects, allow one to confirm the above-made statement, that inorganic lyotropic liquid crystals represent a new and unexplored area, in spite of the fact that they have been known for a long time. In this connection, the aim of the present review is to stimulate studies in this new and interesting field.

References

1 F. Reinitzer, *Sitzungsber. Bayer. Akad. Wiss. Math. Naturwiss. Kl.*, 1886, **94**, 719.
2 O. Lehmann, *Ann. Phys.*, 1985, **56**, 771.
3 A. S. Sonin, *Zh. Strukt. Khim.*, 1991, **32**, 137 (in Russian).
4 Q. Majorana, *Phys. Z.*, 1902, **4**, 145.
5 A. Schmauss, *Ann. Phys.*, 1903, **10**, 658.
6 A. Schmauss, *Ann. Phys.*, 1903, **12**, 186.
7 Y. Bjornstahl, *Philos. Mag.*, 1921, **42**, 352.
8 A. Cotton and H. Mouton, *Ann. Chim. Phys.*, 1907, **40**, 145.
9 W. Heller and H. Zocher, *Z. Phys. Chem.*, 1933, **164**, 365.
10 H. Diesselhorst, H. Freundlich and B. Leonard, *Elster-Geitel-Fortschrift*, 1915, 453.
11 H. Freundlich, *Z. Elektrochem.*, 1916, **22**, 27.
12 H. Diesselhorst and H. Freundlich, *Phys. Z.*, 1915, **16**, 419.
13 W. Reinders, *Kolloid Z.*, 1917, **21**, 161.
14 A. Szegvari, *Z. Phys. Chem.*, 1924, **112**, 295.
15 H. Zocher, *Z. Phys. Chem.*, 1921, **98**, 293.
16 H. Freundlich, F. Stapelfeld and H. Zocher, *Z. Phys. Chem.*, 1925, **114**, 161.
17 H. Freundlich, F. Stapelfeld and H. Zocher, *Z. Phys. Chem.*, 1925, **114**, 190.
18 H. Freundlich, H. Neukircher and H. Zocher, *Kolloid Z.*, 1926, **38**, 48.
19 H. Zocher, *Z. Phys. Chem.*, 1912, **98**, 293.
20 H. Zocher and K. Jacobsohn, *Kolloid Beih.*, 1929, **28**, 167.
21 H. Zocher, *Z. Anorg. Allg. Chem.*, 1925, **147**, 91.
22 H. Zocher and K. Jacobsohn, *Kolloid Z.*, 1927, **41**, 220.
23 J. Jochims, *Kolloid Z.*, 1927, **41**, 215.
24 H. Zocher and C. Torok, *Kolloid Z.*, 1960, **170**, 140.
25 J. Bernal and J. Fankuchen, *Nature*, 1937, **139**, 923.
26 H. Zocher, *Kolloid Z.*, 1954, **139**, 81.
27 H. Zocher and C. Torok, *Acta Crystallogr.*, 1967, **22**, 751.
28 H. Zocher, *Mol. Cryst. Liq. Cryst.*, 1969, **7**, 177.
29 J. Livage, *Chem. Mater.*, 1991, **3**, 578.
30 P. Davidson, A. Garreau and J. Livage, *Liq. Cryst.*, 1994, **16**, 905.
31 W. Biltz, *Ber. Dtsch. Chem. Ges.*, 1904, **37**, 1098.
32 E. Muller, *Z. Chem. Ind. Kolloide*, 1911, **8**, 302.
33 J. Lemerle, L. Nejem and J. Lefebre, *J. Inorg. Nucl. Chem.*, 1990, **42**, 17.
34 W. Prandtl and L. Hess, *Z. Anorg. Allg. Chem.*, 1913, **82**, 103.
35 J. Ketelaar, *Nature*, 1936, 316.
36 J. Ketelaar, *Chem. Weekbl.*, 1936, **33**, 51.
37 H. G. Bachmann, F. R. Ahmed and W. H. Barnes, *Z. Kristallogr.*, 1961, **115**, 110.
38 P. Adelbert, N. Baffier, N. Gharbi and J. Livage, *Mater. Res. Bull.*, 1981, **16**, 669.
39 J. Legendre, P. Adelbert, N. Baffier and J. Livage, *J. Colloid Interface Sci.*, 1983, **94**, 84.
40 P. Adelbert, H. Haesslin, N. Baffier and J. Livage, *J. Colloid Interface Sci.*, 1984, **98**, 478.
41 T. Kamiyama, T. Iton and K. Suzuki, *J. Non-Cryst. Solids*, 1988, **100**, 466.
42 K. Takiyama, *Bull. Chem. Soc. Jpn.*, 1958, **31**, 555.
43 J. Legendre and J. Livage, *J. Colloid Interface Sci.*, 1983, **94**, 75.
44 N. Baffier, P. Adelbert, J. Livage and H. Haesslin, *J. Colloid Interface Sci.*, 1991, **141**, 467.
45 C. Scanchez, J. Livage and G. Lucazeau, *J. Raman Spectrosc.*, 1982, **12**, 68.
46 M. Vandenborre, R. Prost and J. Livage, *Mater. Res. Bull.*, 1983, **18**, 1133.
47 L. Abello and G. Lucaseau, *J. Chim. Phys.*, 1984, **81**, 539.
48 L. Abello, E. Husson, G. Lucaseau and Y. Repelin, *J. Solid State Chem.*, 1985, **56**, 379.
49 J. H. Watson, W. Heller and W. Wojtowicz, *Science*, 1949, **109**, 274.
50 J. Donnet, *Compt. Rend.*, 1948, **227**, 508.
51 J. Donnet, H. Zbinden, H. Benoit, M. Daune, N. Dubois, J. Pouget, G. Scheibling and G. Vallet, *Compt. Rend.*, 1950, **47**, 51.
52 K. Takiyama, *Bull. Chem. Soc. Jpn.*, 1958, **31**, 329.
53 J. Livage, N. Gharbi, M. C. Leroy and M. Michaud, *Mater. Res. Bull.*, 1978, **13**, 1117.
54 W. Heller and W. Wojtowicz, *J. Appl. Phys.*, 1949, **20**, 343.
55 S. Berkman and H. Zocher, *Kolloid Z.*, 1927, **42**, 315.
56 E. V. Generalova, E. L. Kitaeva and A. S. Sonin, *I All-Union conference of lyotropic liquid crystals, Abstracts*, Ivanovo, 1990, p. 38 (in Russian).
57 A. S. Sonin, *Usp. Fiz. Nauk.*, 1987, **152**, 273 (in Russian).
58 Song Ki Chang and Chung In Gae, *J. Non-Cryst. Solids*, 1989, **108**, 37.
59 H. B. Weiser and W. O. Milligan, *Adv. Colloid Sci.*, 1942, **1**, 227.
60 W. O. Milligan and H. B. Weiser, *J. Phys. Colloid Chem.*, 1951, **55**, 490.
61 L. H. Genner and K. H. Storks, *Ind. Eng. Chem. Anal. Ed.*, 1939, **11**, 538.
62 F. J. Ewing, *J. Chem. Phys.*, 1935, **3**, 420.
63 M. S. Goldsztaub, *Bull. Soc. Fr. Mineral.*, 1935, **59**, 348.
64 R. Hocart and J. Lapparent, *Compt. Rend.*, 1929, **189**, 995.
65 P. P. Reichertz and W. J. Yost, *J. Chem. Phys.*, 1946, **14**, 495.
66 H. Zocher and C. Torok, *Kolloid Z.*, 1960, **173**, 1.
67 H. Zocher and C. Torok, *Kolloid Z.*, 1962, **180**, 41.
68 M. Potel, R. Chevrel, M. Sergent, M. Decroux and O. Fisher, *Compt. Rend., Ser. A*, 1979, **288**, 429.
69 M. Potel, R. Chevrel, M. Sergent, J. C. Amici and O. Fiser, *J. Solid State Chem.*, 1980, **35**, 286.
70 J. M. Tarascon, G. W. Hull and F. J. Di Salvo, *Mater. Res. Bull.*, 1984, **19**, 915.

71 J. M. Tarascon, F. J. Di Salvo, C. H. Chen, P. J. Carrol, M. Walsh and L. Rupp, *J. Solid State Chem.*, 1985, **58**, 290.
72 P. Davidson, J. C. Gabriel, A. M. Levelut and P. Batail, *Europhys. Lett.*, 1993, **21**, 317.
73 V. A. Michalev and V. A. Tcherbakov, *Zh. Obshch. Khim.*, 1985, **55**, 1223 (in Russian).
74 V. A. Tcherbakov, L. L. Tcherbakova and B. V. Semakov, *Zh. Strukt. Khim.*, 1974, **15**, 925 (in Russian).
75 V. A. Michalev and V. A. Tcherbakov, *Zh. Strukt. Khim.*, 1985, **55**, 1229 (in Russian).
76 N. V. Kazakov, A. V. Kaznacheev and A. S. Sonin, *Izv. Akad. Nauk SSSR, Ser. Fiz.*, 1991, **55**, 1731 (in Russian).
77 V. A. Tcherbakov and L. L. Tcherbakova, *Radiokhimiya*, 1984, **26**, 708 (in Russian).
78 U. Hofmann, *Angew. Chem., Int. Ed. Engl.*, 1968, **7**, 681.
79 V. A. Druch and A. G. Kossovskaja, *Glinistie minerals. M., Nauka*, 1990 (in Russian).
80 K. Kajiwara, N. Donkai, Y. Hiragi and H. Inagaki, *Macromol. Chem.*, 1986, **187**, 2883.
81 N. Donkai, H. Inagaki, K. Kajiwara, H. Urakawa and M. Schmidt, *Macromol. Chem.*, 1985, **186**, 2623.
82 K. Kajiwara, N. Donkai, Y. Fujiyoshi and H. Inagaki, *Macromol. Chem.*, 1986, **187**, 2895.
83 R. Bradfield and H. Zocher, *Kolloid Z.*, 1929, **47**, 223.
84 A. Buzagh, *Kolloid Z.*, 1929, **47**, 223.
85 H. Zocher and W. Heller, *Z. Anorg. Allg. Chem.*, 1930, **186**, 75.
86 A. L. Mackay, *Mineral. Mag.*, 1960, **32**, 545.
87 A. L. Mackay, *Mineral. Mag.*, 1962, **33**, 270.
88 J. H. Watson and R. R. Cardell, *J. Appl. Phys.*, 1961, **32**, 1641.
89 J. H. Watson and R. R. Cardell, *J. Phys. Chem.*, 1962, **66**, 1757.
90 Y. Maeda and S. Hachisu, *Colloids Surf.*, 1983, **6**, 1.
91 W. Heller, O. Kratky and H. Nowotny, *Compt. Rend.*, 1936, **202**, 1171.
92 K. Coper and H. Freundlich, *Trans. Faraday Soc.*, 1937, **33**, 348.
93 W. Heller, *Compt. Rend.*, 1935, **201**, 831.
94 J. H. Watson, W. Heller and W. Wojitowicz, *J. Chem. Phys.*, 1948, **16**, 997.
95 W. Heller, W. Wojtowicz and J. H. Watson, *J. Chem. Phys.*, 1948, **16**, 998.
96 J. H. Watson, W. Heller and W. Wojtowicz, *J. Chem. Phys.*, 1948, **16**, 999.
97 J. Turkievich and W. Heller, *J. Anal. Chem.*, 1949, **21**, 475.
98 K. Furusawa and S. Hachisu, *J. Colloid Interface Sci.*, 1968, **28**, 167.
99 P. Bergmann, P. Low-Beer and H. Zocher, *Z. Phys. Chem. A*, 1938, **181**, 301.
100 H. Thiele, *Z. Anorg. Allg. Chem.*, 1930, **190**, 145.
101 G. Ruess, *Kolloid Z.*, 1945, **110**, 17.
102 H. Thiele, *Kolloid Z.*, 1948, **111**, 15.
103 P. Gaubert, *Compt. Rend.*, 1922, **174**, 1115.
104 P. P. Von Weimarn, *Zh. Russ. Fiz-Khim. Ova.*, 1908, **40**, 1323 (in Russian).
105 P. P. Von Weimarn, *Kolloid Z.*, 1927, **44**, 279.
106 A. A. Vedenov and E. B. Levchenko, *Usp. Fiz. Nauk*, 1983, **141**, 3 (in Russian).

Feature Article 8/02666A